Geology of the 1:24,000 Roanoke East Quadrangle and investigations of the Long Island Creek Gneiss within the southernmost Appalachians, Alabama and Georgia

by

Rylleigh Paige Harstad

A thesis submitted to the Graduate Faculty of
Auburn University
in partial fulfillment of the
requirements for the Degree of
Master of Science

Auburn, Alabama
August 6th, 2017

Keywords: Roanoke East, Brevard shear zone, Long Island Creek Gneiss, Alleghanian orogeny, southernmost Appalachians, Alabama and Georgia

Approved by

Mark G. Steltenpohl, Chair, Professor of Geoscience
Willis E. Hames, Professor of Geoscience
Haibo Zou, Professor of Geoscience
Clinton I. Barineau, Associate Professor of Geoscience

ABSTRACT

The geology of the 1:24,000 Roanoke East, Alabama, Quadrangle has been determined to be of high mapping priority by the State Geologic Mapping Advisory Committee due to the rapid development along the I-85 corridor west of Atlanta, Georgia. Objectives for this study are: (1) to map and describe lithologies and their distributions; (2) to analyze structures and fabrics; (3) to produce a vector ArcGIS geologic map of the Roanoke East, Alabama, Quadrangle; (4) to characterize the Long Island Creek Gneiss through both geochronological and geochemical analyses, and; (5) to synthesize the geologic history. The key findings are seven-fold. (1) The lithologies of the Jacksons Gap Group within the Roanoke East Quadrangle are not easily divided into separate, mappable units as a result of their lithological similarities and their inter-gradational nature. The current author divides the lithologies of the Jacksons Gap Group within the Roanoke East Quadrangle into two main lithofacies types: a structurally lower section defined mostly by garnetiferous-graphitic-quartz-biotite schists and phyllites interlayered with micaceous quartzites; and an upper section of variably graphitic, garnetiferous-sericite-chlorite schists and phyllites, with no interlayered quartzites. The Long Island Creek Gneiss intrudes these units. (2) The lithologies of the Jacksons Gap Group within the Roanoke East Quadrangle are also not easily distinguishable from lithologies of the immediately adjacent units (the Emuckfaw Group and schists within the Waresville Schist). Outcrops of cataclasites defining the Abanda and Katy Creek faults

bounding the Jacksons Gap Group were not observed and, hence, placing the upper and lower boundaries of the package proved to be a difficult task. (3) The current author defines the upper limit of the Emuckfaw Group within the Roanoke East Quadrangle based on the presence/lack of metagraywackes, which occur together with rare, thin amphibolites. I also have defined the lower limit of the Waresville Schist by the occurrence of amphibolites, interpreting them to be part of the metavolcanics of the Dadeville Complex. This contrasts with the placement of the same contacts by workers in Georgia, who instead place these amphibolites within lithologies of the Brevard shear zone. (4) The Long Island Creek Gneiss that intrudes the Jacksons Gap Group does not appear to cross over the boundaries of the Brevard shear zone within the area of the Roanoke East Quadrangle. (5) Early D_1 fabrics and lithologic contacts are locally truncated at the Katy Creek fault where syn- to late-D_1 fabrics parallel it, implying the juxtaposition of the Dadeville Complex and Jacksons Gap Group during a syn- to late-D_1/M_1 event. An inverted metamorphic gradient along the Katy Creek fault may have been formed as a result of down-heating that occurred during the emplacement of the hot Dadeville Complex on top of the cooler Jacksons Gap Group. (6) The age of Rock Mills Granite Gneiss remains to be constrained geochronologically, but it is younger than the 466 Ma Waresville Schist it intrudes (VanDervoort et al., 2017). (7) Based on available evidence, the Long Island Creek Gneiss is a highly fractionated melt emplaced at 293.1 +/- 5.3 Ma during the end of the period of Alleghanian plutonism spanning between ~330 and 295 Ma (Lin, 2015), placing a maximum on the timing of right-slip movement along the Brevard shear zone.

ACKNOWLEDGMENTS

There are several individuals and groups to whom I am indebted; without their support over the past two years, this project would not have been possible. First and foremost, my advisor Dr. Mark Steltenpohl has been the best mentor I could have asked for, not only for my research but also for my career as a whole- thank you for always having your door open for me. I would not have made it to where I am without Dr. Clinton Barineau, who has been fundamental in my development as a geologist and a constant source of inspiration over the past five years. Dr. Joshua Schwartz was a critical element in the success of my geochronology, and I thank him for his persistence. Dr. Karen Tefend's and Dr. Randy Kath's contributions to the understanding of the Long Island Creek Gneiss are most appreciated. I would also like to thank Dr. Chong Ma and Dr. Stefanie Brueckner for the incredible assistance with understanding and interpreting my geochronologic and geochemical data.

I want to thank my family and friends for the constant support over the years as I have chased my crazy rock dreams- your believing in me has helped me climb every mountain I've encountered. My field assistant John Whitmore has been incredible over the past two years, and I thank him for the many conversations and support. My former office-mate and now boyfriend Dane VanDervoort has been my rock the last two years, and I thank him for believing in me when I didn't and for helping cultivate my mind as a geologist through endless discussions over many beers. Finally, I want to thank all those

organizations and groups that have provided funding for my endeavors: the United States Geologic Survey, the Geological Society of America, the Alabama Geological Society, and the Department of Geosciences Advisory Board. Of course, it also goes without saying that I owe this wonderful opportunity to Auburn University- War Eagle!

TABLE OF CONTENTS

List of Figures

List of Tables

List of Plates

INTRODUCTION

The Roanoke East Quadrangle is located within the Piedmont province of the southern Appalachians in east-central Alabama, and encompasses rocks from two major terranes, the eastern Blue Ridge (EBR) and the Inner Piedmont (IP), that are separated by the Brevard fault zone (BFZ). Within the BFZ is a group of related lithologies of uncertain affinity, called the Jacksons Gap Group (JGG) (Bentley and Neathery, 1970). The Long Island Creek Gneiss (LICG) is the most continuously exposed granitic body intruding lithologies of the BFZ of Alabama and Georgia, yet the unit is poorly understood and remains to be geochronologically and geochemically characterized in Alabama. As a whole, the Piedmont of Alabama includes metasedimentary, metavolcanic, and metaplutonic rocks that formed as a result of the processes associated with the Taconic (Ordovician), Acadian-Neoacadian (Devonian-Mississippian), and Alleghanian (Carboniferous) orogenic events (Bentley and Neathery, 1970; Hatcher, 1989, 2005; VanDervoort et al., 2015). Previous regional reconnaissance mapping of rocks in and surrounding the Roanoke East Quadrangle provided a limited amount of structural and metamorphic data (Bentley and Neathery, 1970; Medlin and Crawford, 1973; Higgins et al., 1988). The Roanoke East Quadrangle lies west of Atlanta, Georgia near the I-85 corridor, a main transportation route between Montgomery, Alabama and Atlanta, Georgia, in an area where development is expected (Steltenpohl, 2014). Detailed geologic mapping has been limited in the Roanoke East Quadrangle, and is needed for

several reasons: (1) urban planning and development; (2) for Source Water Protection studies as required by the Alabama Department of Environmental Management; (3) for identifying and clarifying the presence of natural resources; (4) to address issues concerning the geologic evolution of the Appalachian orogenic belt, particularly in regard to the Brevard fault zone (Steltenpohl, 2014), and; (5) to further constrain the LICG and its role in the tectonic evolution of the southernmost Appalachians.

Location and Physiographic Setting

The 1:24,000 Roanoke East, Alabama, Quadrangle (Latitudes: 33°07’30”N and 33°15’N; Longitudes: 85°15’W and 85°22’30”W) lies within Randolph County in the Piedmont province of the southern Appalachians in east-central Alabama, and just crosses into Heard County, Georgia to the northeast (Figures 1 and 2). The cities and communities in the Roanoke East Quadrangle are Roanoke, Rock Mills, Bacon Level, Lime, Center Chapel, Springfield, Paran, High Shoals, and Wehadkee within Randolph County. Elevations range from 660 feet along the banks of Wehadkee Creek southeast of Rock Mills, to more than 1200 feet on hills east of High Shoals in the northwestern corner of the quadrangle. Topographic features include rolling hills accompanied by prominent ridges formed by the differential weathering of more silica-rich units (Bentley and Neathery, 1970). Streams within the quadrangle drain into Lake Martin, located approximately 40.5 miles (65 km) to the southwest of Roanoke, Alabama.

Geologic Setting

The eastern Blue Ridge is the structurally lowest terrane in the study area (Figures 1 and 2), and consists of two major metasedimentary packages, the Wedowee and Emuckfaw groups. To the northwest, the Wedowee Group is located structurally above the Hollins Line fault and has been traditionally described as being composed of variably graphitic garnet mica schist interlayered with quartzite, biotite paragneiss (metawacke), feldspathic garnet mica schist, amphibolites, and is intruded by Devonian to Carboniferous metagranitoids (Bentley and Neathery, 1970; Neathery and Reynolds, 1975; Allison, 1992; Stowell et al., 1996; Schwartz et al., 2011; Tull et al., 2012). The Emuckfaw Group overlies the Wedowee and is bound by the Brevard fault zone to the southeast. The Emuckfaw is a sequence of undifferentiated metagraywackes, graphitic and aluminous schists, quartzites, and amphibolites that is intruded by Ordovician- to Silurian-aged plutons (Zana Granite and Kowaliga Gneiss) (Neathery and Reynolds, 1975; Hawkins, 2013; Sagul, 2016). Traditionally, the dextral strike-slip Alexander City fault (ACF) has been interpreted as the boundary between the Wedowee and Emuckfaw Groups (Figure 2) (Neathery and Reynolds, 1975; Steltenpohl et al., 2013), while many workers interpret it as a normal fault that doesn't define the entire boundary between the two units (Drummond, 1986; Allison, 1992; Drummond et al., 1997; Tull et al., 2012; Harstad and Barineau, 2014; Barineau et al., 2015; Roop-Eckart and Barineau, 2015). The rocks of the eastern Blue Ridge have most commonly been described as the outboard slope/rise facies of the Neoproterozoic Iapetus-facing Laurentian margin, and some workers have suggested that a distal back-arc basin evolved on top of it (Steltenpohl, 2005; Tull et al., 2012, 2014).

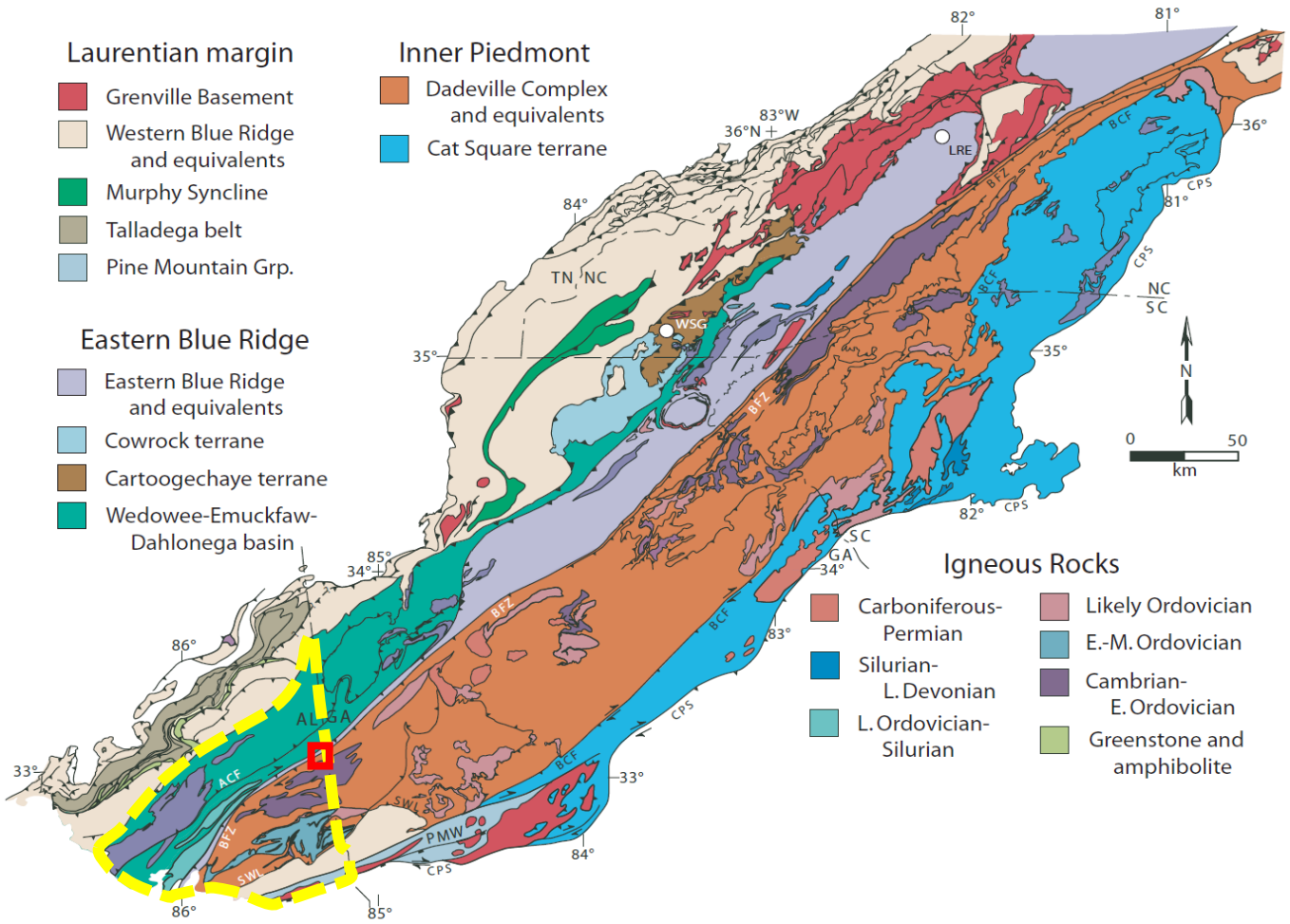

Figure 1: Geologic map of the southern Appalachians, with the limits of Figure 2 outlined in the yellow dashed line and the approximate location of the Roanoke East, Alabama, Quadrangle in red. Modified after Merschat et al., 2010 (VanDervoort and Steltenpohl, 2015).

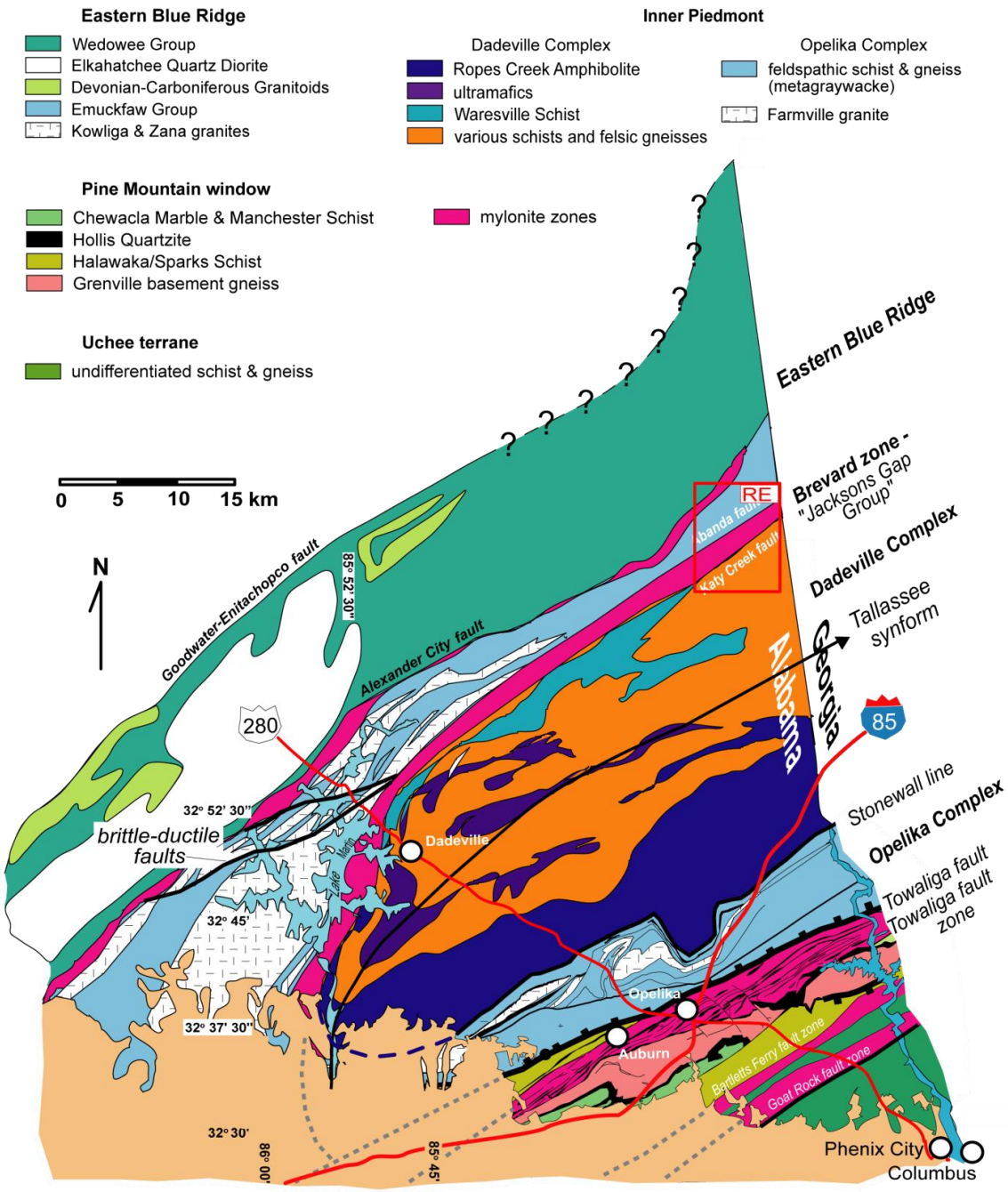

Figure 2: Geologic map of the Alabama Piedmont (from Osborne et al., 1988, Steltenpohl, 2005, and Steltenpohl et al., 2013) showing the location of the Roanoke East (RE) Quadrangle (outlined in red).

To the southeast, the Brevard fault zone separates metasedimentary and metaplutonic rocks of the eastern Blue Ridge from metavolcanic and metaplutonic rocks of the Inner Piedmont (Figures 1 and 2) (Bentley and Neathery, 1970). The Brevard fault zone has been the focus of intense study and debate among southern Appalachian geologists for over five decades, but is typically interpreted as a polyphase fault zone that initially formed in response to Acadian-Neoacadian thrusting, overprinted by Alleghanian brittle-plastic dextral strike-slip shearing (Vauchez, 1987; Hatcher, 1989, 2005; Steltenpohl et al., 2013).

Bounded by the Abanda fault to the northwest and the Katy Creek fault to the southeast (Figure 2), the Jacksons Gap Group defines the lithologies of the Brevard fault zone in Alabama. The Jacksons Gap Group is a narrow zone (up to 2.8 km wide) of strongly to weakly deformed metasiliciclastic and metapelitic rocks (Bentley and Neathery, 1970; Sterling, 2006; White, 2007). VanDervoort and Steltenpohl (2015) recognized that in the type locality of the Abanda Fault (Abanda, Alabama, Wadley South 7.5" quadrangle), widely spaced C-planes and high angles between them and complementary S-planes in phyllonites imply relatively lower degrees of shear stress.

The Jacksons Gap Group is generally described as a sequence of undifferentiated graphitic button-schists, phyllites, sericitic phyllites, quartzites, and graphitic quartzites that commonly are phyllonitized and mylonitized (Bentley and Neathery, 1970). Lithologies of the Jacksons Gap Group are compatible with an origin along the ancient rifted Laurentian margin, similar to the Emuckfaw Group, although the former is of a distinctly shallower marine depositional setting. Sterling et al. (2005) reported the rare presence of rare continental-rift meta-basalts within the Jacksons Gap Group. The

Jacksons Gap Group in Alabama typically lacks granitic intrusive rocks, causing it to contrast sharply with rocks above and below it (i.e., the Dadeville Complex and the eastern Blue Ridge, respectively). The Long Island Creek Gneiss (LICG), however, is the most continuously exposed granitic gneiss sheet affected by shearing within the Brevard fault zone. The LICG is typically a titanite-epidote-biotite-quartz-feldspar gneissic granite that is medium- to coarse-grained and moderately- to well-foliated and lineated; locally the granite contains muscovite (Crawford et al., 1999). The only age reported for the LICG is a Rb-Sr isochron age of 460 Ma (Sinha and Higgins, 1987), which likely is not a robust age date, given problems of mobility of these elements. An objective of the current thesis is to re-date the LICG using more modern U-Pb methods.

The Dadeville Complex of the Inner Piedmont terrane is the structurally highest tectonostratigraphic unit in the field area, and occurs directly southeast of the Brevard fault zone. The Dadeville Complex comprises interlayered schist, metaquartzite, and amphibolite (Waresville Formation), layered to massive amphibolite (Ropes Creek Amphibolite), tonalitic gneiss (Waverly Gneiss), aluminous schist (Agricola Schist), and two different suites of felsic intrusives (the Camp Hill Gneiss and the Rock Mills Granite Gneiss) (Bentley and Neathery, 1970). VanDervoort et al. (2017) report dates for the Waresville Formation at 466.6 ± 5.6 Ma, the Ropes Creek Amphibolite at 458.6 ± 5.6 Ma, the Waverly Gneiss at 461 ± 11 Ma, and the Camp Hill Gneiss at 487 ± 11 Ma; an age of 460 ± 4 Ma for the Camp Hill Gneiss is reported by Farris et al. (2015). To the southeast of the Dadeville Complex is the Opelika Complex (Figure 2), which initially was considered part of the Inner Piedmont as well. However, several workers have documented that the Opelika Complex correlates to rocks of the eastern Blue Ridge and

even perhaps parts of the Jacksons Gap Group, and it is now believed that only the Dadeville Complex is of Inner Piedmont affinity (Bentley and Neathery, 1970; Grimes and Steltenpohl, 1993; Keefer, 1992; Steltenpohl et al., 2005; Abrahams, 2014; Tull et al., 2014; VanDervoort et al., 2015).

Previous Investigations

Earlier investigations of the rocks in and surrounding the Roanoke East Quadrangle were primarily concerned with economic endeavors, describing gold occurrences, mine locations, mineralogy, and brief accounts of the regional geology (Tuomey, 1858; Phillips, 1892; Adams, 1930; Park, 1935; Pardee and Park, 1948). Adams (1926, 1930) first described the Wedowee formation, and correlated it with the rocks of the Brevard zone, interpreting them as altered Wedowee formation. Bentley and Neathery (1970) performed a significant amount of regional work and delimited the Brevard fault zone and Inner Piedmont, providing a foundation for geologic studies by subsequent workers. In contrast with Adams' work, Bentley and Neathery (1970) designated the Wedowee formation as the Wedowee Group. They also defined the rocks between the Wedowee Group and the Brevard fault zone as the Heard Group, and the associated felsic intrusives as the Zana Granite and Kowaliga Gneiss. Bentley and Neathery (1970) did not specify a type section for lithologies of the Brevard fault zone, but they did describe it as a zone of deformation and cataclasis, bounded by the Abanda fault to the north and the Katy Creek fault to the south. Structurally above the Brevard fault zone, the same authors divided the Inner Piedmont into the Dadeville Complex and the Opelika Complex, and defined several different mappable units (e.g., the Waresville

Formation, Agricola Schist, Camp Hill Gneiss, Ropes Creek Amphibolite, and the Boyds Creek Mafic Complex). These authors also suggested that the southern Appalachian Piedmont is allochthonous along a west-directed thrust comprising the Brevard fault zone, along with faults framing the Pine Mountain basement window (i.e., Towaliga, Bartletts Ferry, and Goat Rock fault zones). A similar conclusion was later proposed by The Consortium for Continental Reflection Profiling (COCORP), based on their seismic-reflection profiling (Cook et al., 1979).

Following the initial work of Bentley and Neathery (1970), the rocks of the eastern Blue Ridge were renamed the Heard Group (Neathery and Reynolds, 1973), the Emuckfaw formation (Neathery and Reynolds, 1973), and then the Emuckfaw Group (Raymond et al., 1988). Subsequent work focused on characterizing the development and timing of emplacement of the Zana and Kowaliga intrusive bodies within the Emuckfaw, employing mapping as well as geochemical and geochronological techniques. Over the years, several authors have reported that the Zana and Kowaliga are genetically related (Muangonoicharoen, 1975; Stoddard, 1983; Hawkins, 2013). An age of 461 ± 12 Ma for both the Zana and Kowaliga (using multi-grain U-Pb zircon analysis) was reported by Russell (1987), along with a Rb-Sr whole-rock ages of 437 Ma and 395 Ma, respectively, with uncertainties on the order of ± 100 Ma. Hawkins (2013) employed Secondary Ionization Mass Spectrometry (SIMS) U-Pb isotopic analysis on zircons from the Kowaliga Gneiss and reported a crystallization age of 440 Ma. More recently, Sagul (2016) obtained ages on both the Zana and Kowaliga suggesting that these plutons formed during a period of magmatism from ~480 to ~455 Ma.

Wielchowsky (1983) described rocks within and adjacent to the Brevard fault zone from the Alabama-Georgia state line southwest to Jacksons Gap, Alabama as a "lithologically distinctive" metasedimentary sequence within a shear zone that flattens with depth. This is compatible with the COCORP seismic profile that suggests the fault rooted at depth into the southern Appalachian master décollement (Cook et al., 1979). Further work reported in Auburn University student theses between 1988 and 2015 have made significant contributions to the understanding of the geology and gold/precious metal occurrences within the Jacksons Gap Group through detailed geologic mapping, structural analysis, and geochemical and geochronological analysis (Johnson, 1988; Keefer, 1992; Grimes, 1993; Reed, 1994; McCullars, 2001; Sterling, 2006; White, 2007; Hawkins, 2013; Abrahams, 2014; Singleton and Steltenpohl, 2014; Poole, 2015; VanDervoort, 2015).

TECTONOSTRATIGRAPHY

Tectonostratigraphic terranes exposed on the Roanoke East Quadrangle comprise, from northwest to southeast, the eastern Blue Ridge, the Jacksons Gap Group, and the Inner Piedmont. Eastern Blue Ridge units in this study are the Wedowee and Emuckfaw groups, the latter of which is intruded by the Kowaliga Gneiss, occupying the northwestern half of the quadrangle. Metasedimentary rocks of the Jacksons Gap Group are intruded by the Long Island Creek Gneiss and occur as an approximately 1.25-mile wide band exposed diagonally across the middle portion of the quadrangle. The Inner Piedmont comprises the Waresville Schist and Rock Mills Granite Gneiss of the Dadeville Complex. Units shown on Plate 1 are described below, from the southeast to the northwest, or from structurally highest to structurally lowest order. Unit names and symbols listed below correspond to those found on Plate 1.

The current author has recognized features and relationships associated with faults and/or shear zones exposed on the Roanoke East Quadrangle, and also those reported for quadrangles along strike to the southwest and northeast, that lead her to suggest modifications be made for some of their names. The gradational nature of lithologies along the boundary between the Wedowee and Emuckfaw groups on the Roanoke East quad is associated with variably developed phyllonitic shear zones but these do not require a faulted relationship between these units. Combined with observations reported for shearing but not fault displacement along this boundary to the northeast and

southwest (Muangonoicharoen, 1975; Barineau and Tull, 2012; Harstad and Barineau, 2014; Roop-Eckart and Barineau, 2015), the current author prefers using the term Alexander City shear zone for these distributed shears. Likewise, field and structural studies along the Brevard fault zone in Alabama clearly document that phyllonites and mylonites are not simply restricted to the confines of the Jacksons Gap Group being partitioned by its flanking faults, the Abanda and the Katy Creek, respectively to the northwest and southeast (e.g., Sterling, 2006; Hawkins, 2013; Abrahams, 2014; Poole 2015; and VanDervoort, 2015). Lithologies at the top of the Emuckfaw Group are indistinguishable from parts of the lower Jacksons Gap Group within the Roanoke East Quadrangle, and previous workers have had similar problems placing the boundary between the two units (White, 2007; Reynolds and Steltenpohl, 2009; Hawkins, 2013). For these reasons, the current author prefers using the term Abanda shear zone. In contrast, the Katy Creek fault juxtaposes rocks of two terranes, the Jacksons Gap Group and the Dadeville Complex arc (Taconic), and, therefore, the term Katy Creek fault is retained. Given the preponderance of distributed shear zones occurring outside of the Jacksons Gap Group, however, the current author favors the term Brevard shear zone rather than Brevard fault zone, and hence the former is used below.

Due to the Roanoke East Quadrangle being located partially on the Alabama-Georgia state line, consideration was taken for the correlation (or lack thereof) of various faults/shears as previously reported between the two states. Beginning in the northwest of the quadrangle, the Alexander City shear zone roughly correlates with the Omaha fault described by workers in Georgia (Crawford and Kath, 2015), yet the Roopville fault was not observed during the current study. The Abanda shear zone correlates with the

Chattahoochee fault described by workers in Georgia. However it is placed much further to the southeast than the Chattachoochee fault due to a differing interpretation of the boundaries of the Brevard shear zone between Alabama (based on lithology; i.e., the JGG) and Georgia (based on structure). The Long Island fault reported in Crawford and Kath (2015) is not noted as a fault/shear in Alabama, although the Long Island Creek Gneiss is clearly stretched and sheared. The Katy Creek fault correlates directly with the Clairmont fault of Georgia.

Lithostratigraphic Units

Inner Piedmont/Dadeville Complex

The structurally highest terrane in the study area is the Inner Piedmont, represented within the Roanoke East Quadrangle by the Waresville Schist and the Rock Mills Granite Gneiss of the Dadeville Complex. The Waresville Schist is described as a package of mostly metamorphosed mafic and felsic metavolcanics, and the Rock Mills Granite Gneiss is a granitic metaplutonic body. These lithologies make up the remaining southern half of the Roanoke East Quadrangle where, typical of the nature of the Dadeville Complex, outcrops are more difficult to find.

Rock Mills Granite Gneiss (Idrm)

The Rock Mills Granite Gneiss is named for large pavement exposures (Figures 3 and 4) in Rock Mills, Randolph County, Alabama, which is located within the Roanoke East Quadrangle (Raymond et al., 1988). The Rock Mills Granite Gneiss is a well-foliated, medium- to coarse-grained granitic gneiss containing biotite, muscovite, quartz,

Figure 3: Photograph of the large pavement exposures and waterfall on Wehadkee Creek formed by the Rock Mills Granite Gneiss in Rock Mills, Alabama for which the unit was named. View is looking north-northwest (33°9'30.96", -85°17'21.84").

Figure 4: Another photograph of the pavement exposures in Rock Mills, Alabama on Wedhadkee Creek. View is looking southeast, from the same location as Figure 3.

potassium feldspar, and varying minor amounts of epidote and garnet. In fresh exposures, the Rock Mills Granite Gneiss commonly is white to light tan in color. Where weathered, aligned platy minerals retain the metamorphic foliation within the soil, which is a light tan color. The Rock Mills Granite Gneiss typically exhibits spheroidal weathering patterns (Figure 5) that contributes to the gentle, rolling hill topography of the southern portion of the quadrangle (Figure 6).

Waresville Schist (Idws)

The Waresville Schist is mostly a bimodal metavolcanic sequence of interlayered mafic and felsic schists, and thinly banded to massive amphibolite (Figures 7 and 8). The mafic layers consist of very fine- to fine-grained amphibole-bearing schist and banded amphibolites (Figure 9), and are interpreted to be metamorphosed basalt lava flows. The felsic layers consist of a fine- to medium-grained schist containing varying amounts of quartz, plagioclase, potassium feldspar, and sericite; locally the schist contains minor amounts of pyrite. These felsic schists are interpreted to represent metamorphosed tonalitic lava flows. In fresh exposures, the mafic layers are a deep green to dark gray to black color, and the felsic layers are a white to light tan or light gray color. Mafic layers weather to a deep brick-red soil, and the felsic layers weather to a light tan soil. Along with these lithologies, the Waresville Schist also contains aluminous feldspar-rich schists that are locally difficult to distinguish from the schists of the Jacksons Gap Group. These schists are interlayered with the felsic and mafic lithologies previously described, and are interpreted as either metamorphosed ash or volcaniclastic deposits, but they are not distinguishable at the scale of Plate 1.

Figure 5: Photograph of the Rock Mills Granite Gneiss, displaying its typical spheroidal weathering pattern. Also note the subhorizontal foliation, typical of the Rock Mills Granite Gneiss. View is looking east-southeast (33°12'13.644", -85° 15'25.308").

Figure 6: Photograph of an open field within the southern portion of the Roanoke East Quadrangle, showing the gentle rolling hills resulting from weathering of the underlying Rock Mills Granite Gneiss. View is looking east-southeast (33°8'37.68", -85°15'19.8").

Figure 7: Photograph of interlayered mafic and felsic schists of the Waresville Schist. View is looking to the east (33°12'4.32", -85°17'42").

Figure 8: Interlayered mafic and felsic schists of the Waresville Schist, near the contact with the Jacksons Gap Group where it becomes more difficult to distinguish between the two units (Waresville Schist and Jacksons Gap Group). View is looking to the southwest (33°9'50.076", -85°22'0.588").

Figure 9: Photograph of banded amphibolite within the Waresville Schist. View is looking to the north (33°11'15.72", -85°17'30.12").

Jacksons Gap Group/Brevard Shear Zone

Structurally above and separated from the eastern Blue Ridge by the Abanda shear zone, the rocks of the Jacksons Gap Group define the Brevard shear zone within the Roanoke East Quadrangle. These lithologies occupy an approximately 2 kilometer wide band that stretches across the middle of the quadrangle, from the western edge to the northeastern corner. Within the current area, the lithologies of the Jacksons Gap Group have been divided into three different mappable units: garnetiferous schist, micaceous quartzite, and sericite-chlorite phyllite. The Long Island Creek Gneiss intrudes these units.

Long Island Creek Gneiss (Licg)

Within the Roanoke East Quadrangle, the Long Island Creek Gneiss is a medium- to coarse-grained, moderately- to well-foliated epidote-muscovite-biotite-quartz-feldspar gneissic granite. It is intensely foliated and lineated with stretched grains, and it appears to be a simple gneiss with dark and light bands. The Long Island Creek Gneiss is a roughly tabular body that stretches across the middle portion of the Brevard shear zone and is stretched/sheared along the Katy Creek fault. In fresh exposures, it occurs as smooth, whale-back outcrops underlying ridges (Figure 10) and it weathers to a light tan soil.

Sericite-Chlorite Phyllite (JGscp)

At the structural top of the Jacksons Gap Group, a sericite-chlorite phyllite dominates and occurs as a fine- to medium-grained, well-foliated, locally graphitic

phyllite that contains varying amounts of garnet, quartz, muscovite, sericite, and chlorite. It is locally interlayered with garnetiferous schists that are identical to those seen within the Garnetiferous Quartz Schist of the Jacksons Gap Group. Close to the Katy Creek fault, and near the immediately adjacent Waresville Schist, it can be difficult to distinguish between the two units. In fresh outcrops, it is light olive-green to silvery-gray, and it weathers to a deep brick-red soil.

Garnetiferous Quartz Schist (JGgqs)

At the structural base of the Jacksons Gap Group within the study area, lithologies are dominated by a locally graphitic, fine- to medium-grained garnetiferous biotitie-sericite-quartz schist. In fresh outcrops, the Garnetiferous Quartz Schist is typically light gray to light tan, and weathers to a light tan to light reddish soil that contains weathered-out mica fish and garnets (Figure 11). Kinematic indicators include asymmetric mica fish, which tend to weather out into 'buttons,' rolled garnet porphyroblasts, sigmoidal-shaped feldspar porphyroclasts, and asymmetrically folded quartz ribbons. The lithologies are difficult to distinguish from the immediately adjacent graphitic schists of the Emuckfaw Group.

Micaceous Quartzite (JGmq)

Found only towards the northeastern portion of the quadrangle, also at the base of the Jacksons Gap Group, is a fine- to medium-grained, well-foliated, micaceous quartzite that contains varying amounts of muscovite, biotite, sericite, quartz, and feldspar. In fresh exposures, it expresses itself in a 'blocky' fashion, and typically weathers to a light tan to

Figure 10: Photograph of an outcrop of steeply dipping Long Island Creek Gneiss in an open field. View is looking to the northeast (33°11'42.36", -85°20'44.16").

Figure 11: Photograph of moderately weathered Garnetiferous Quartz Schist of the Jacksons Gap Group, displaying typical soil colors and mica buttons on the ground. View is looking to the east (33°14'20.04", -85°16'13.8").

light reddish soil (Figure 12). Within the Roanoke East Quadrangle, this lithology only had one mappable band, but was found interlayered with the Garnetiferous Quartz Schist (JGgqs) in other locations in bands no more than approximately 0.5 meters thick.

Eastern Blue Ridge

The eastern Blue Ridge is the structurally lowest terrane in the region and, within the Roanoke East Quadrangle, is represented by the Wedowee Group, the Emuckfaw Group, and the Kowaliga Gneiss. These rocks occur structurally below the Abanda shear zone, which marks the structural bottom of the Brevard shear zone.

Kowaliga Gneiss (Ekg)

Within the Roanoke East Quadrangle, the Kowaliga Gneiss occurs as small tabular to lenticular pods, up to 2 kilometer long (along strike) and ~0.5 kilometers wide, of a strongly foliated granitic gneiss that intrude the schists, metawackes, and amphibolites of the Emuckfaw Group. The Kowaliga Gneiss is a medium- to coarse-grained augen gneiss containing quartz, potassium feldspar, plagioclase, biotite, and muscovite. The foliation is defined by the alignment of biotite and muscovite grains that drape the more competent potassium feldspar augen. Fresh rocks occur as either large pavement exposures or in rounded boulders. The Kowaliga Gneiss typically weathers to a light tan soil.

Emuckfaw Group (Eem)

The remainder of the eastern Blue Ridge within the Roanoke East Quadrangle is

Figure 12: Photograph of Micaceous Quartzite from the Jacksons Gap Group, exhibiting the typical ‘blocky’ outcrop and light tan to light red soil. View is looking to the north (33°14'21.984", -85°16'16.392").

occupied by the Emuckfaw Group, originally named for exposures along Emuckfaw Creek in Tallapoosa County, Alabama (Neathery and Reynolds, 1975). In the current study area, the Emuckfaw Group consists of an undifferentiated sequence of locally graphitic and garnetiferous muscovite-biotite-quartz-feldspar schist (sub-millimeter unidentified opaques also occur locally), fine-grained muscovite-biotite-quartz-feldspar metawacke, and thin, rare fine-grained banded amphibolite that are intruded by the Kowaliga Gneiss (Ekg). Like the Wedowee Group, these rocks also record a relatively high degree of dextral shear strain (Figures 13 and 14). In outcrop, the Emuckfaw Group varies from a bronzy (vermiculitic)- to silvery-gray sheen and weathers to a tan to reddish-orange sandy, muscovite- and garnet-rich soil. The metawackes are more competent than the surrounding schists, and tend to protrude in outcrops where the schist has been more deeply weathered, and may also be responsible for the formation of moderately strong topographic ridges within the Emuckfaw Group (see Plate 1). Outcrops of the amphibolites very rarely are fresh, and usually have been deeply weathered to a deep ochre-red color with a porous, punky, brick-bat appearance (Figure 15). Metawackes within the Emuckfaw Group vary anywhere between several centimeters to several meters in thickness, whereas the amphibolites are rarely more than roughly 20 centimeters thick. Locally, small pods (no larger than one foot in the longest dimension) of stretched and dismembered, coarse-grained, biotite-muscovite-feldspar-quartz granitic intrusives occur within the schists of the Emuckfaw Group (Figure 16).

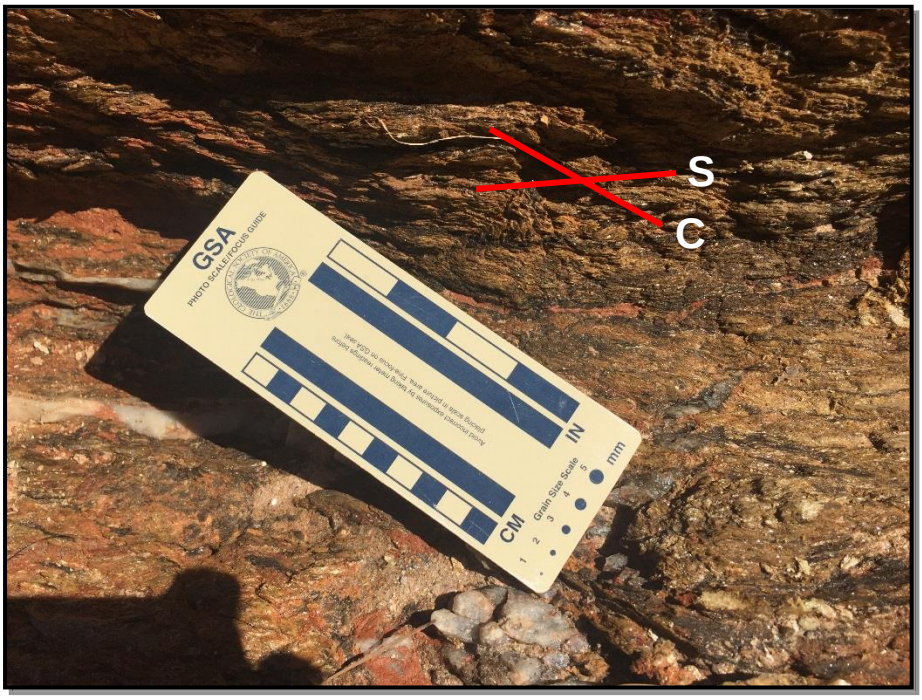

Figure 13: Photograph of a well-developed S-C fabric within the schists of the Emuckfaw Group, indicating a dextral sense of shear. View looking to the southeast, down dip (33°14'35.16", -85°20'38.4").

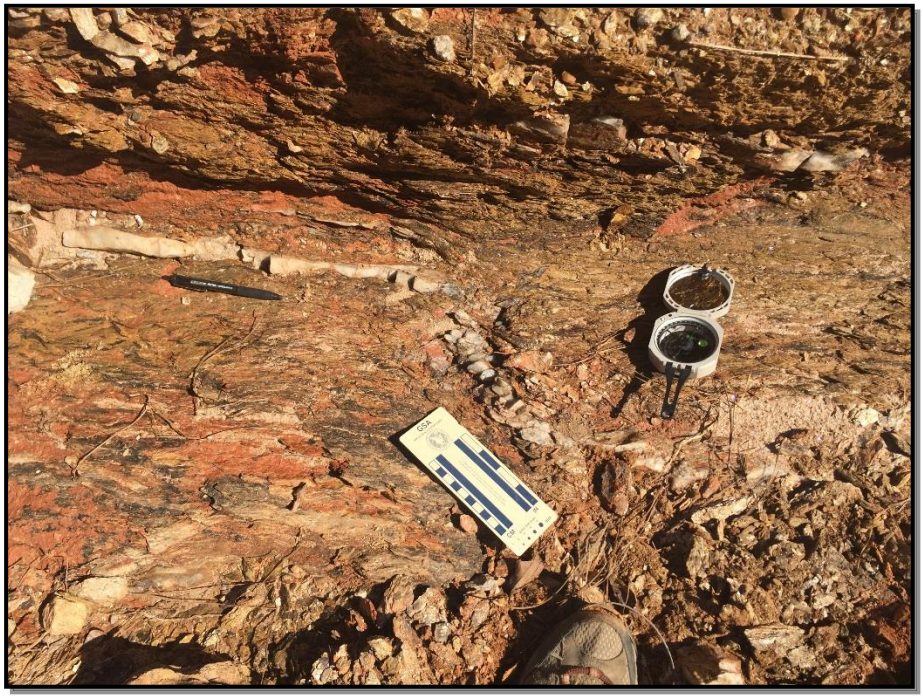

Figure 14: Photograph of an open Z-fold in a quartz vein within the Emuckfaw Group, again indicating a dextral sense of shear. View is looking toward the southeast, down dip (33°14'35.16", -85°20'38.4").

Figure 15: Photograph of weathered banded amphibolite within the Emuckfaw Group, exhibiting the typical porous, punky brick-bat appearance. View is looking northeast (33°14'10.32", -85°18'8.28").

Figure 16: Photograph of a sheared, medium-grained schist in the Emuckfaw Group, with small, lens-like pods of felsic intrusives. Note- north arrow on scale is not pointing in proper direction. View is looking to the north (33°14'56.4", -85°21'23.76").

Wedowee Group (Ewe)

The Wedowee Group was named for exposures near Wedowee, Alabama (Neathery and Reynolds, 1975), and occupies a very small portion of the northwestern corner of the Roanoke East Quadrangle. The Wedowee Group in the current study area comprises only a graphitic garnetiferous muscovite-biotite-quartz-feldspar schist. Other workers (i.e., VanDervoort, 2015) have documented the occurrence of a banded to massive amphibolite (Beaverdam Amphibolite in the uppermost parts of the Wedowee Group). However, in the current study area, only minor amounts of float and outcrops of this lithology were found. The schists within the Wedowee Group locally record a relatively high degree of dextral shear strain, preserved in well-developed S-C fabrics. In outcrop, the schist is silvery-gray and weathers to an orange/reddish-orange soil. The contact between the Wedowee Group and the Emuckfaw Group, which is gradational over a ~100 meter section, was placed on the basis of graphite content, with the Wedowee Group being highly graphitic in the study area and the Emuckfaw Group being only variably graphitic.

METAMORPHISM

Three tectonometamorphic events have been documented in the southern Appalachians. The first at ~480 Ma (Taconian) is documented locally as high grade (eclogite and granulite facies) in parts of the eastern Blue Ridge of North Carolina (Abbott and Raymond, 1984, 1997; Absher and McSween, 1986; Raymond et al., 1989; Adams et al., 1995). The second event was at ~350 Ma (Neoacadian; Hatcher 1989, 2005) and the third at ~330 Ma (early or eo-Alleghanian), both under amphibolite facies and were accompanied by local shearing between ~300 and 285 Ma (late Alleghanian) (Steltenpohl and Kunk, 1993; Dennis and Wright, 1997; Carrigan et al., 2001; Kohn, 2001; Bream, 2002, 2003; Cyphers and Hatcher 2006; Stahr et al., 2006; Hames et al., 2007; McClellan et al., 2007; McDonald et al., 2007). Observations within the Roanoke East Quadrangle are compatible with this metamorphic history, where the rocks of the Dadeville Complex experienced Taconian effects, and the eastern Blue Ridge, Jacksons Gap Group, and Inner Piedmont appear to have gone through a period of lower greenschist- to upper amphibolite-facies, Barrovian-style prograde metamorphism (Neoacadian/early Alleghanian), followed by a second extensive retrogressive middle to upper greenschist-facies metamorphic event (Muangnoicharoen, 1975; Wielchowsky, 1983; Johnson, 1988; Steltenpohl et al., 1990; Reed, 1994; Sterling, 2006; Hawkins, 2013; Abrahams, 2014; Singleton and Steltenpohl, 2014; Poole, 2015; VanDervoort et al., 2015, 2017) (Figure 17).

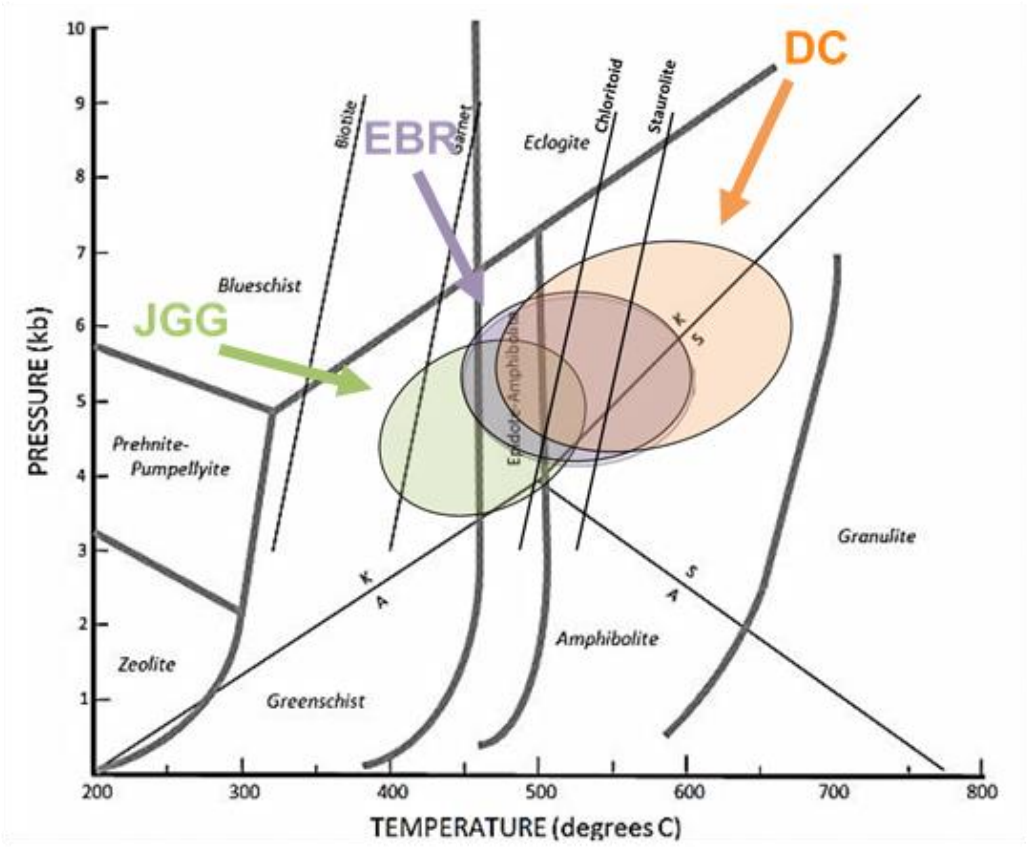

Figure 17: Conditions suggested for peak metamorphism. Eastern Blue Ridge – purple, Jacksons Gap Group – green, and Dadeville Complex – orange (modified from Hawkins, 2013, and Poole, 2013).

Guthrie and Dean (1989) reported prograde mineral assemblages of kyanite + staurolite + muscovite + biotite + garnet + plagioclase + quartz within the Emuckfaw Group in Alabama, suggesting a lower to middle amphibolite-facies peak of metamorphism (Holdaway, 1971; Ernst, 1973). These same authors also interpreted the replacement of hornblende by actinolite and chlorite in rocks of the Emuckfaw Group as having occurred under middle to upper greenschist-facies retrogressive metamorphic conditions. Within the Kowaliga Gneiss, deformational microstructures in quartz and feldspar grains indicate subgrain rotation, bulging recrystallization, and grain boundary migration, compatible with lower amphibolite-facies conditions (Hawkins, 2013) (Figure 17).

The Jacksons Gap Group is dominated by a prograde mineral assemblage of muscovite + biotite + garnet + quartz, but this assemblage is not diagnostic of metamorphic grade. Along the structural top of the Jacksons Gap Group, in rocks adjacent to the Dadeville Complex, assemblages containing kyanite and garnet are documented; for example, directly southwest of the study area, staurolite + kyanite + sillimanite indicate middle amphibolite-facies peak metamorphic conditions (Johnson, 1988; Sterling, 2006). The Jacksons Gap Group presents an anomaly in that it contains primary sedimentary structures including cross stratification, graded bedding, and conglomerates, suggesting low degrees of metamorphism and strain (Bentley and Neathery, 1970; Sterling, 2006; Poole, 2015). The current investigation within the Roanoke East Quadrangle is consistent with the observation that metamorphic grade increases from greenschist-facies at the base of the Jacksons Gap Group to lower to middle amphibolite-facies at the top (Figure 17).

Within the Dadeville Complex, the Waresville Schist and Rock Mills Granite Gneiss contain prograde assemblages of garnet + biotite + muscovite + plagioclase, compatible with middle amphibolite-facies metamorphism, similar to findings by VanDervoort (2015) (Figure 17). Retrogressive greenschist- to lower amphibolite-facies mineral assemblages are not dominant, but observed as the alteration of hornblende to actinolite and chlorite. These observations are consistent with observations of the same rocks made by Johnson (1988), Steltenpohl and Moore (1988), Steltenpohl et al. (1990), Goldberg and Steltenpohl (1992), Reed (1994), Drummond et al. (1997), Sterling (2006), Abrahams (2014), Steltenpohl and Singleton (2014), Poole (2015), and VanDervoort (2015).

Recently, evidence for metamorphism during the Taconic (Cambrian to Early Ordovician) was recognized by VanDervoort et al. (2015) within rocks of the Dadeville Complex (Agricola Schist) of the Inner Piedmont. They report a prominent zircon-age population in their detrital data set at ~480 Ma with Th/U values <0.1, which they interpret as metamorphic overgrowth. This appears to be the first reported record of Taconic metamorphism in the southernmost Appalachians in Alabama. Specific assemblages supporting Taconian metamorphism in the Dadeville Complex of the current study were not conclusively documented based strictly on field observations.

STRUCTURE

Within the rocks underlying the Roanoke East Quadrangle, structural observations indicate that they have experienced and retain the evidence of at least four deformational events, D_1 through D_4. Table 1 is a summary of each of these deformational events. Structural and fabric elements produced as a result of a particular event are designated with the same subscript; for example: S_1, L_1, and F_1 formed during D_1; S_2, L_2, and F_2 formed in D_2; and so on. All structural measurements are imbedded as data files in the ArcGIS map).

D_1 was associated with the formation of the principle metamorphic assemblages and fabrics found in rocks of the study area. While not observed in the Roanoke East Quadrangle, workers in the surrounding areas have documented the occurrence of primary sedimentary structures (i.e., conglomerates, upward fining sequences and cross-bedding) within siliciclastics of the Jacksons Gap Group, which define a primary bedding (S_0) that otherwise is transposed into the S_1 foliation, resulting in a composite S_0/S_1 fabric (Sterling, 2006; Poole, 2015). Peak, M_1, metamorphic conditions (lower greenschist- to amphibolite-facies) resulted in the formation of the dominant regional foliation (S_1), which is defined by the parallel alignment of phyllosilicate and inequant mineral grains. M_1 is interpreted as having occurred during Neoacadian (Late Devonian-early Mississippian) orogenesis. The primary composite S_0/S_1 fabric has an average strike and dip of N40˚E, 43˚SE in rocks of the Roanoke East Quadrangle (Figure 18).

Table 1. Summary of deformational events in the Roanoke East, Alabama, Quadrangle.

Deformational Phases	Structural Elements	Description
	S_0	Bedding - Compositional layering
* D_1	M_1	Regional prograde dynamothermal metamorphism of the EBR, JGG, and DC (Acadian; Devonian-Mississippian)
	S_1	Regional foliation (schistosity and gneissosity)
		Early mylonitic movement along the BSZ
		Syn- to late-peak metamorphic Katy Creek fault movement
	L_1	Inequant mineral elongation lineation
D_2	M_2	Retrogressive reactivation of the Katy Creek fault (Alleghanian; Carboniferous)
		Early movement along the Abanda and Alexander City shears
	F_2	Tight to isoclinal, intrafolial folding of S_0/S_1
		Late-F_2 folding of the Tallassee synform
	S_2	Local transposition of S_1 into S_2 in the JGG
		Composite S-C mylonitic fabric indicating oblique dextral-normal movement
D_3	M_3	Upper greenschist-facies reactivation of the Abanda and Alexander City faults (Alleghanian; Carboniferous)
	F_3	Asymmetric folds associated with movement along the Abanda fault
	S_3	Composite S-C mylonitic fabric indicating oblique dextral-normal movement along the Abanda and Alexander City shears
	L_3	Mineral lineation within the LICG, constraining timing of movement on BSZ
D_4		Brittle reactivation of the Alexander City fault and BSZ (Late Carboniferous to Jurassic)

* Middle Ordovician (Taconic) metamorphism recently has been documented in the Dadeville Complex (VanDervoort et al., 2015), although associated structures and fabrics are cryptic. Structures and fabrics observed in the Dadeville Complex within the Roanoke East Quadrangle did not reveal any new observations to identify pre-D_1 (Taconian) effects.

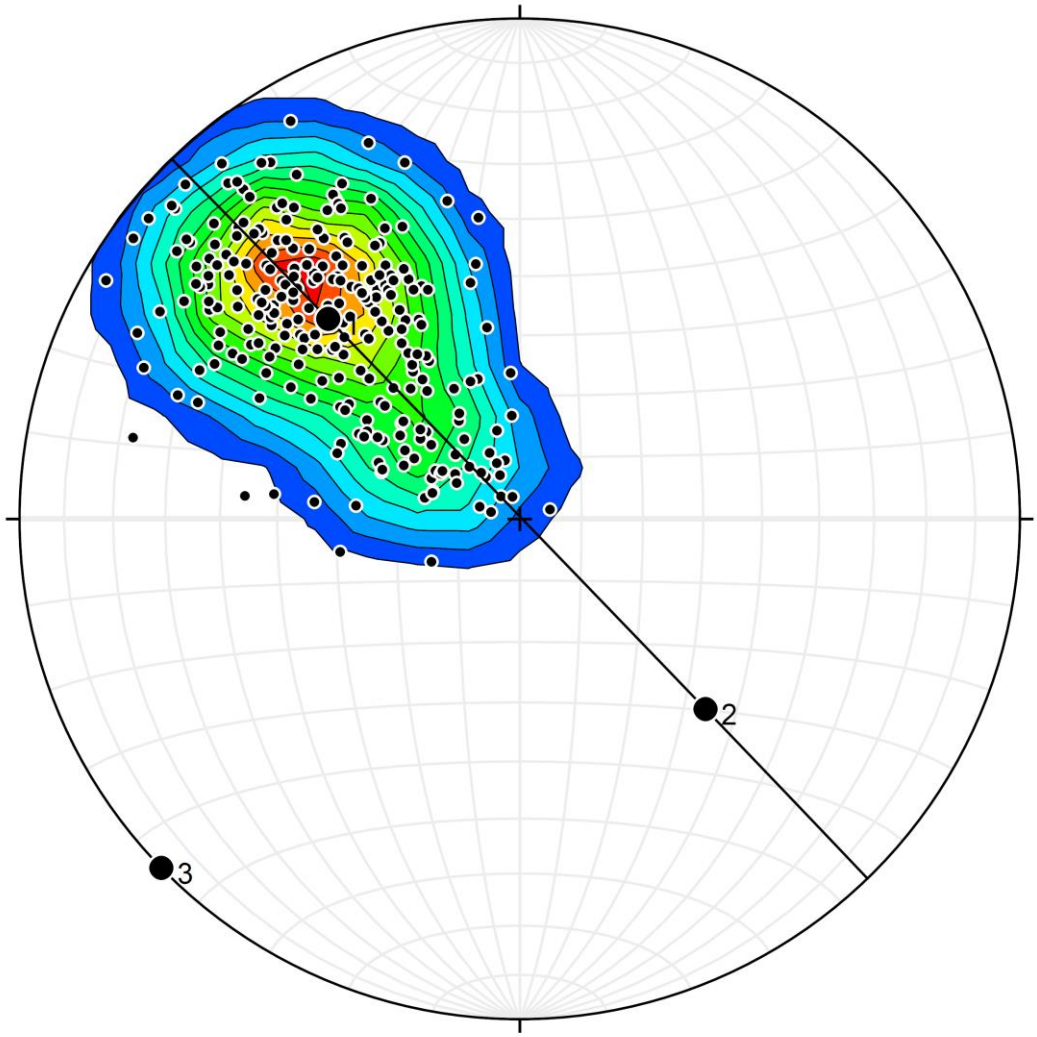

Figure 18: Lower hemisphere stereographic projection of poles (contoured) to S_0/S_1 foliation (C-planes, small black dots, N=289). Average strike and dip of foliation (black dot 1 is the pole to this average) – N40˚E, 43˚SE. Black dot 2 – beta axis; plunge and bearing 46.3˚, S44.3˚E. Black dot 3 – Pi axis; plunge and bearing 0.3˚, S46˚W. Black line – best fit pi girdle; strike and dip N44˚W, 89.7˚NE.

The Katy Creek fault is interpreted to be a D_1 structure. Fault rocks observed along this fault within and outside of the Roanoke East quad locally show evidence for retrograde right-slip shearing. However, in other localities, the structures are cryptic and parallel the metamorphic foliation, implying early- or syn-metamorphic development (Steltenpohl et al., 1990; Grimes, 1993; Sterling, 2006; Abrahams, 2014; Poole, 2015; VanDervoort, 2015). Clear truncations of major units within the Dadeville Complex are observed at map-scales all along the Katy Creek fault. The occurrence of Taconic metamorphism in the hanging-wall Dadeville Complex, combined with a lack of Taconic effects recognized within the footwall Jacksons Gap Group, requires substantial displacement along the Katy Creek fault (VanDervoort and Steltenpohl, 2015). Studies southwest of the Roanoke East quad (Singleton and Steltenpohl, 2014; Poole, 2015) document that the Katy Creek fault juxtaposes higher-grade rocks (i.e., Dadeville Complex) atop distinctly lower-grade rocks (Jacksons Gap Group). This implies an inverted metamorphic gradient formed as a result of Neoacadian down-heating from thrust emplacement of the hot Dadeville Complex upon the cooler Jacksons Gap Group.

The second deformational event (D_2) deformed and retrograded earlier-formed mineral assemblages, fabrics, and structures under lower amphibolite- to upper greenschist-facies conditions. The alignment of retrogressive chlorite and sericite defines the S_2 foliation, with the associated L_2 lineation being defined by the preferred orientation of retrograde inequant mineral grains, and tends to be collinear with L_1. F_2 folds are typically defined as microscopic to mesoscopic, tight to open folds of S_1 that are on trend with F_1 folds, and are coincident with regional, long-wavelength macroscale synforms and antiforms (Steltenpohl et al., 1990). The shallow northeast-plunging Tallassee

synform was produced by folding during D_2 deformation; the west limb is defined by the Jacksons Gap Group and rocks immediately adjacent in the eastern Blue Ridge, and the core is defined by the Dadeville Complex.

D_2 shear zones contain variably developed S-C composite planar fabrics with retrograde assemblages and microstructures reflecting lower-amphibolite- to upper-greenschist facies deformational conditions. The D_2 shear zones are distributed across the study area but are concentrated within the Jacksons Gap Group (Brevard shear zone). They overprint the Katy Creek fault and record early-stage movement along the Alexander City and Abanda shear zones (Table 1). S-C fabrics formed during D_2 indicate a dextral, strike-slip sense of movement, with slip-lines having an average plunge and bearing of 05˚, S45˚W (Figure 19).

The third deformational event (D_3) is represented by prominent retrograde, lower greenschist-facies, composite S-C and S-C-C' fabrics that indicate oblique- dextral-normal movement along the Abanda shear zone. Shear zones associated with D_2 and D_3 are interpreted as corresponding to an array of Alleghanian dextral strike-slip shear zones that extend from the hinterland to as far west as the Goodwater-Enitachopco fault (Steltenpohl et al., 2013). Generally, C-planes for the D_2 shears are more closely spaced and the S- and C-planes have lower angles between them than do the D_3 S-C planes. L_3 observed within the Long Island Creek Gneiss (Licg) also is interpreted to have formed during this event, providing a maximum age of ~293 Ma for the timing of movement on the Brevard shear zone.

The final deformational event (D_4) is recorded within cataclasites along the northwestern side of the Alexander City and Abanda shear zones that overprint earlier

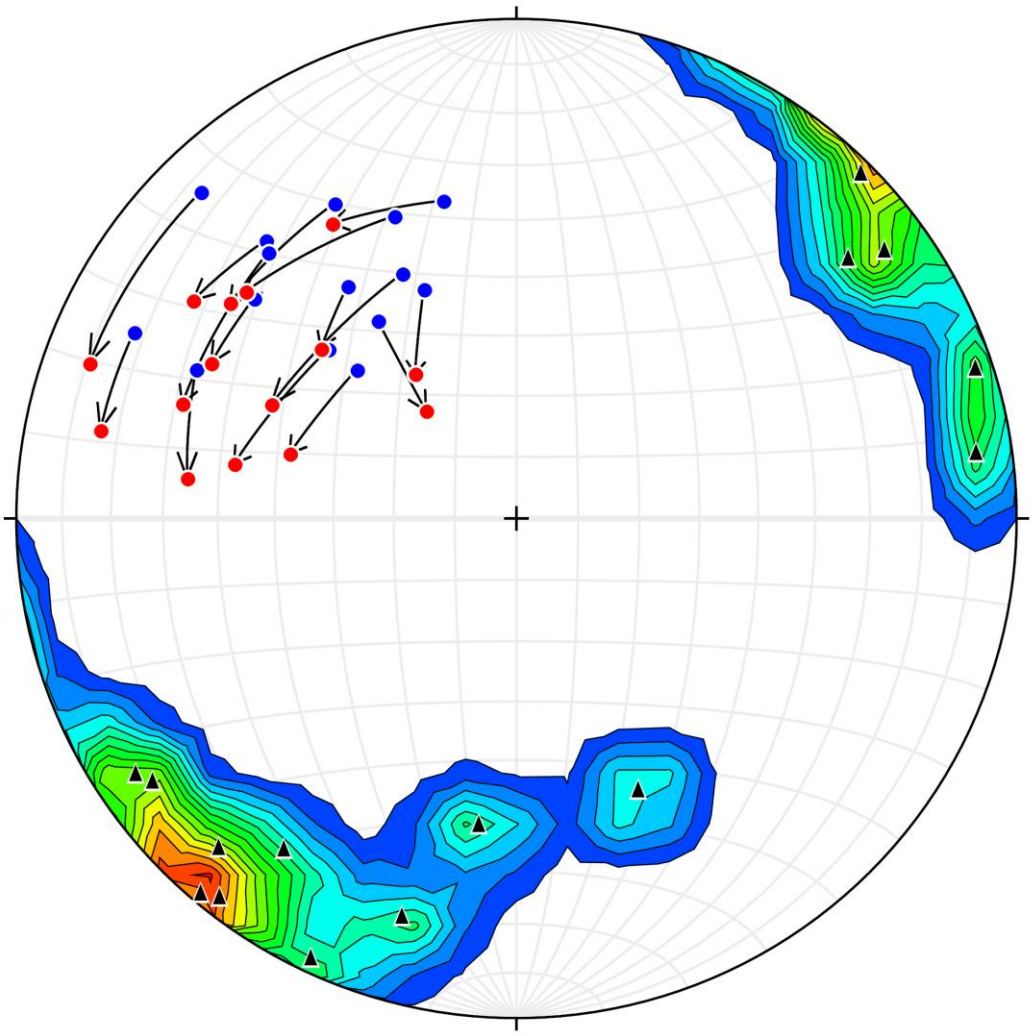

Figure 19: Lower hemisphere stereogram of S-C pairs (black arrows) and slip-lines (black triangles) associated with the Brevard shear zone (N=15). Poles to C-planes are unornamented end of arrows (blue dots) and poles to S-planes are the tip of the arrows (red circles).

fabrics and structures. While these cataclasites were not observed to crop out within the Roanoke East Quadrangle, other workers have described them as non-foliated, very fine- to fine-grained siliceous cataclasites with thin cross-cutting quartz veins (Poole, 2015; VanDervoort and Steltenpohl, 2015). These cataclasites are interpreted as representing the supra-ductile-brittle reactivation of the Alexander City and Abanda shear zones (Steltenpohl et al., 2013). These, along with similar structures throughout the southern Appalachian orogen, are interpreted to reflect the Mesozoic rifting of Pangea (Garihan and Ranson, 1992; Garihan et al., 1993).

GEOCHRONOLOGY AND GEOCHEMISTRY OF THE LONG ISLAND CREEK GNEISS

The Long Island Creek Gneiss (LICG) is the most continuously exposed granitic body intruding the Brevard shear zone and Eastern Blue Ridge of Alabama and Georgia. The LICG is a tabular, medium- to coarse-grained and moderately- to well-foliated and lineated titanite-epidote-biotite-quartz-feldspar granitic gneiss (Figures 20 and 21). Due to the very high feldspar content of the LICG, weathering yields a characteristic light yellow-colored soil, leading to the term "Yellow Dirt Gneiss" as it is known for exposures in Yellow Dirt, Georgia. The LICG has been mapped for nearly 150 km along strike and notably, it can be traced across the zone of most intense shearing within the Brevard shear zone. There is no apparent offset where it is crossed by the individual strands of the zone, but it is stretched roughly parallel to the Brevard zone trend. The gneiss also possesses a variably developed foliation. Both the foliation and lineation appear to be more well-developed along the perimeters of the body and less prevalent within the core, as is expected with syn-kinematic intrusions, but more detailed mapping and strain analysis is needed to further confirm this.

Crystal-plastic mylonitic textures (Figures 22 and 23) are prevalent in the unit (e.g., deformation twins, strain-related myrmekite, and asymmetric mica fish), and it clearly was intruded prior to or synchronous with Brevard zone shearing. Most all primary igneous structures that had previously existed have been erased as they were not

Figure 20: Outcrop of the LICG, looking down-dip of the well-developed foliation. Top of the photo is to the southeast (33˚11’42.36”, -85˚20’44.16”).

Figure 21: Outcrop of the LICG, showing dextrally folded and sheared mylonitic layers. View is to the southeast (33˚11’42.36”, -85˚20’44.16”).

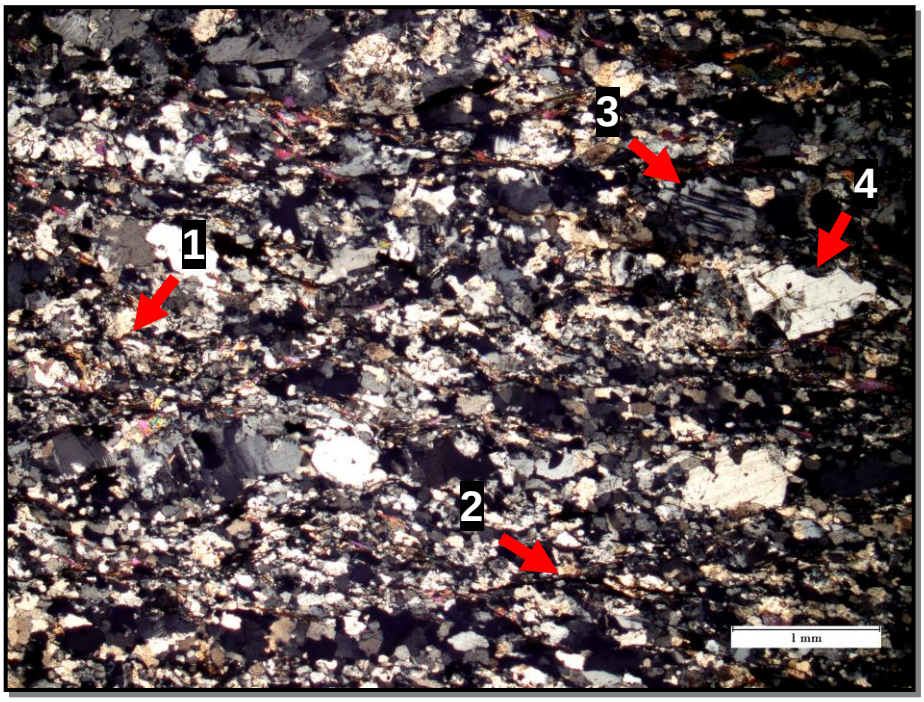

Figure 22: Photomicrograph of the LICG under XPL, showing crystal-plastic mylonitic textures; (1) minor strain-related myrmekite, (2) asymmetric mica fish, (3) deformation twins, and (4) deeply embayed feldspar. Section is cut parallel to elongation lineation and parallel to mylonitic foliation.

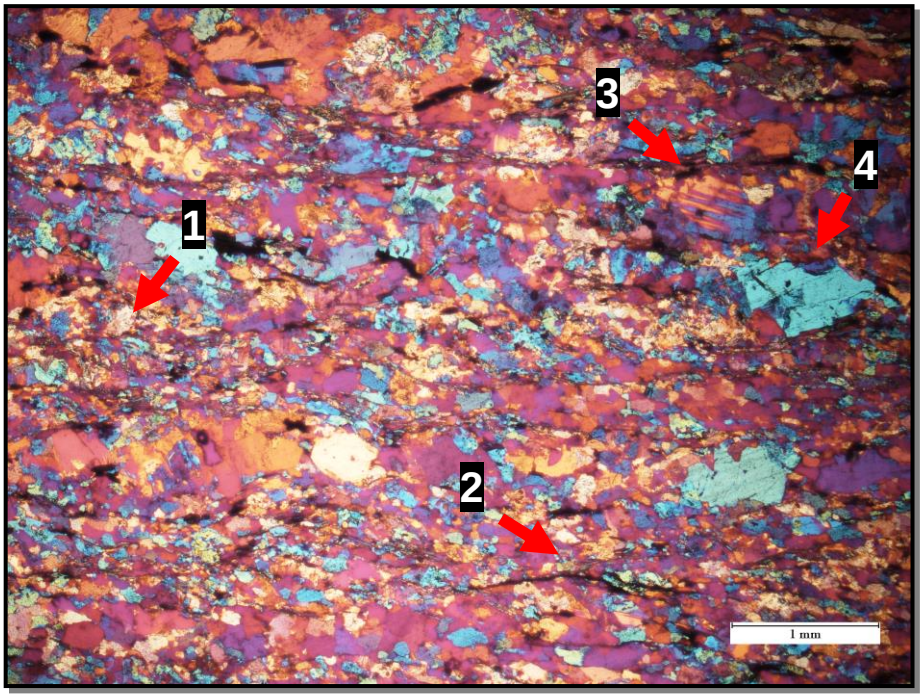

Figure 23: Same view as Figure 22 (same labels), but with the gypsum plate inserted in order to enhance appearance of deformation features.

found in thin sections of the LICG, although zoned zircons and larger-than-matrix feldspar grains (phenocrysts?) likely reflect the igneous heritage. Quartz exhibits undulose extinction, lobate grain boundaries, and minor subgrain development. Bands of quartz generally contain relatively coarse-grained quartz with more curved to straight boundaries between them (see bottom areas of figures 22 and 23) indicating grain-boundary reduction recrystallization (GBRR), which contrasts sharply with retrograde "quartz ribbons" that so commonly characterize the retrograde mylonites of the Brevard zone (e.g., Grimes and Steltenpohl, 1993, and Sterling, 2006). Overall, the quartz microstructures reflect relatively high temperatures of deformation exceeding ~600C (Simpson and Schmid, 1983; Scholz, 1988; Hirth and Tullis, 1994; Tullis, 2002; Passcier and Trouw, 2005). Feldspars exhibit tapering deformation twins, bulging recrystallization, deep embayment, and minor amounts of strain-related myrmekite. Like the quartz microstructures, feldspars have microstructures contrasting sharply with those typically observed for retrograde Brevard zone mylonites. Instead of occurring as porphyroclasts with internally deformed cores and finely recrystallized rims with distinct tails (i.e., sigma- and/or delta-type porphyroclasts), LICG feldspars stand out as larger grains set in the finer-grained matrix with little or no notable core-mantle structures indicating GBRR far exceeded rotational recrystallization, which again suggests relative high deformation temperatures that exceeded ~600C (Tullis, 1983, 2002; Simpson and Schmid, 1983; Tullis and Yung, 1992; Passchier and Trouw, 2005). These temperatures for deformation exceed conditions associated with the Alleghanian retrograde metamorphism and mylonitization (i.e., a middle to upper greenschist-facies event; Grimes and Steltenpohl, 1993; Steltenpohl and Kunk, 1993; Sterling, 2006; Steltenpohl et

al., 2013). Based on the field relations and the microstructural observations supporting near- to sub-magmatic conditions of mylonitization, the current author interprets the LICG to have been emplaced under syn- to late-syn-kinematic conditions.

Despite its importance to Brevard zone evolution, surprisingly little is known about the LICG both in terms of its geochemistry and its age, so its role in the development of the southern Appalachians is not well understood. The only age reported for the LICG had been a Rb-Sr whole-rock isochron-age of ~460 Ma (Sinha and Higgins, 1987), and no published geochemical data exists on the granite. In order to characterize the magmagenesis and timing of the granite, samples of the LICG were collected from exposures within both Alabama and Georgia for geochemical and geochronological studies.

Geochronology

One sample (RRE-15) of the LICG from the Roanoke East, Alabama, Quadrangle was selected for geochronological analysis of zircons using U-Pb age-dating methods. The sample location can be seen in Figures 24 and 25, and in Appendix I. The outcrop from which RRE-15 was collected was located in a roadside hill (both sides of the road) just north of White Crossroads. Strike and dip of the foliation at this location is N45˚E, 60˚SE. The sample selected was the most ideal compared to other outcrop locations of the LICG within the quadrangle due to the lesser degree of deformation observed and the pristine quality (‘freshness’) of the rock, both crucial to obtaining zircons ideal for dating the timing of magmatic crystallization.

Initial zircon separation took place at Columbus State University under the

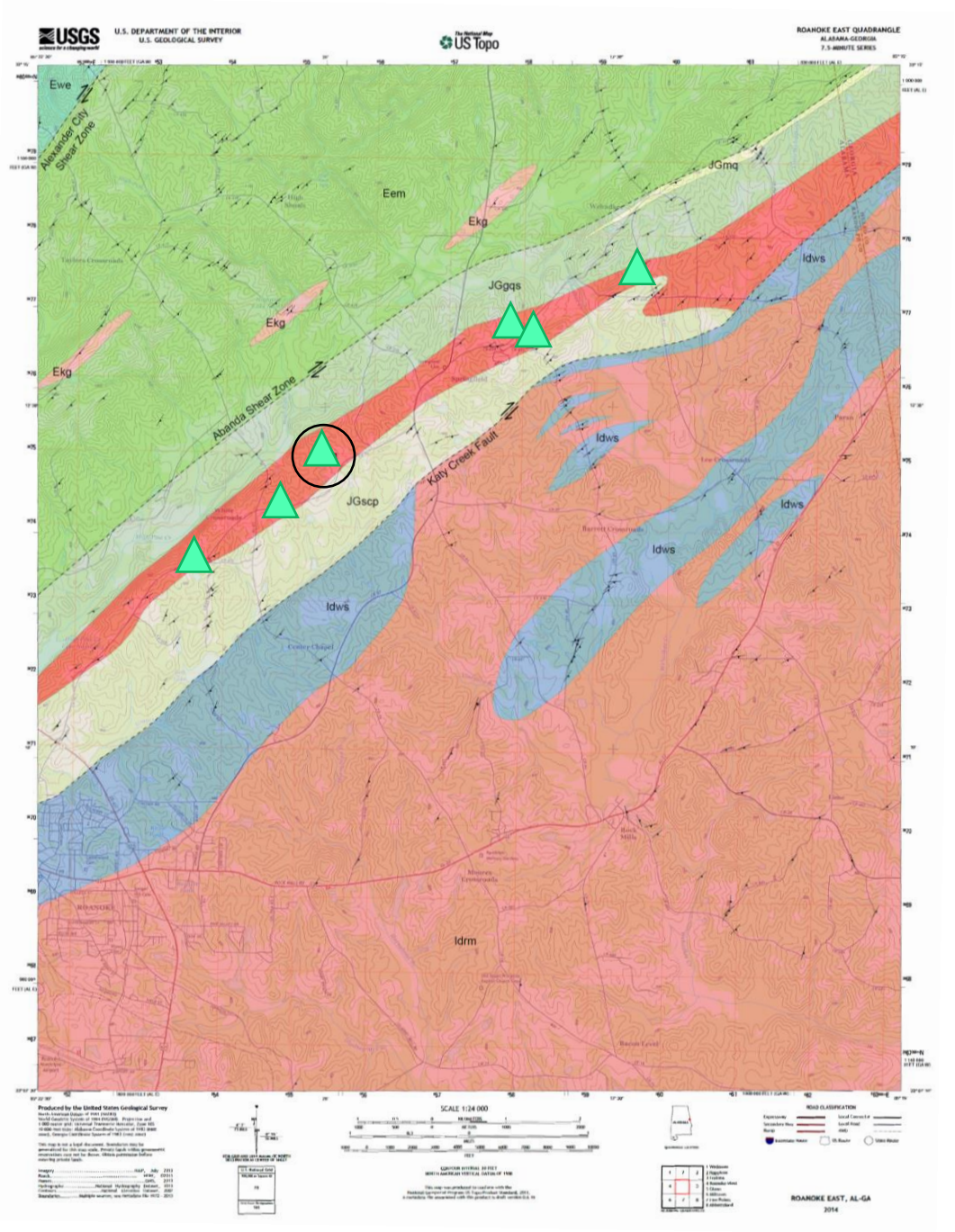

Figure 24: Geologic map of the Roanoke East, Alabama Quadrangle. Triangles represent geochemical sample locations; the black circle denotes the sample location for geochronological analyses.

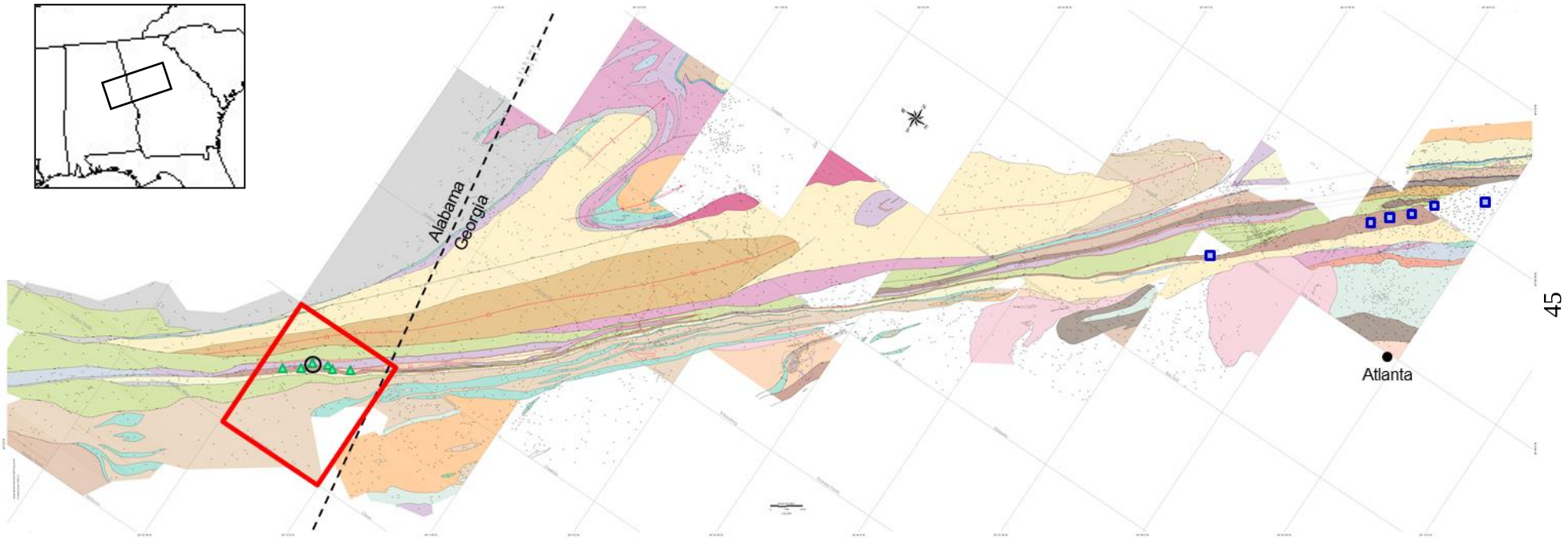

Figure 25: Detailed geologic map along the BSZ from Abanda, Alabama to north of Atlanta by Crawford and Kath (2015). The location of the Roanoke East, Alabama, Quadrangle in Figure 24 is outlined by the red box. The LICG is indicated by the brown, roughly tabular unit. Sample locations for geochemical analyses by Dr. Karen Tefend are denoted by blue squares; note that multiple samples were collected at some locations.

supervision of Dr. Clint Barineau. The sample was first crushed using a jaw crusher, and was then put through a 500 micron sieve. The portion of sample < 500 microns was passed through a spiral panner in order to initially separate lighter materials (including fine dust) from the heavier, denser materials. The 'heavies' were passed through a Frantz magnetic separator to remove as much magnetic material as possible. Heavy (high density) liquid separation occurred at Auburn University under the supervision of Dr. Mark Steltenpohl. Portions of the non-magnetic sample were processed using methylene iodide (MEI; density of 3.32 g/cm^3) in order to separate zircon from all other materials (including apatite) until all of the sample was processed. Zircons were hand-picked under a high power microscope and sent to Dr. Joshua Schwartz at California State University, Northridge for mounting, imaging and final analysis using LA-SF-ICP-MS methods. All data were plotted using Isoplot 3.75 (Ludwig, 2012).

The final results, including standards that were analyzed, are indicated in Appendix II. Individual zircons were labeled on the basis of their morphology (anhedral or euhedral). A relative probability plot of all analyses can be seen in Figure 26, displaying a prominent peak at ~290 Ma and minor peaks at ~400-500 Ma, ~600 Ma, and ~1000 Ma. A weighted average of all analyses <400 Ma (25 out of 32 analyzed zircons) was calculated, yielding an age of 293.1 ± 5.3 Ma (Figure 27). A Terra-Wasserburg diagram of the more pristine, euhedral zircons (Figure 28) yields an intercept age at 291.0 ± 5.5 Ma, which is consistent with the weighted average seen in Figure 27; discordance is attributed to the presence of older, inherited zircons. Originally the author sought to explore the hypothesis that the LICG is potentially related to the Ordovician Zana and

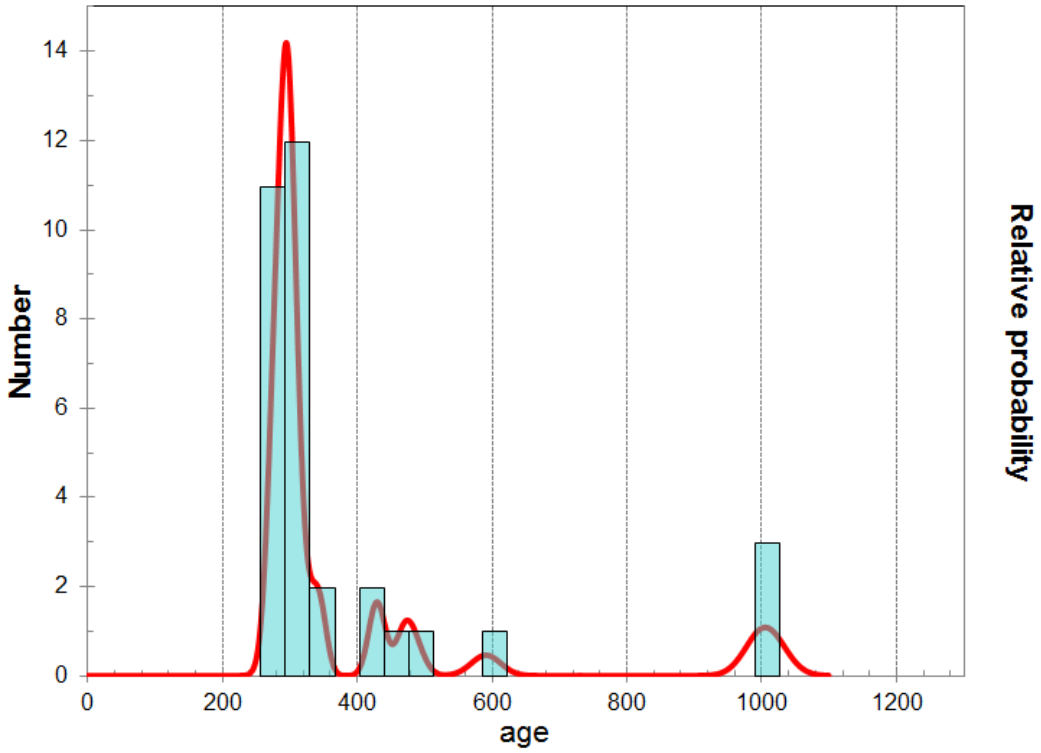

Figure 26: Relative probability plot of all U-Pb analyses of zircons from the LICG.

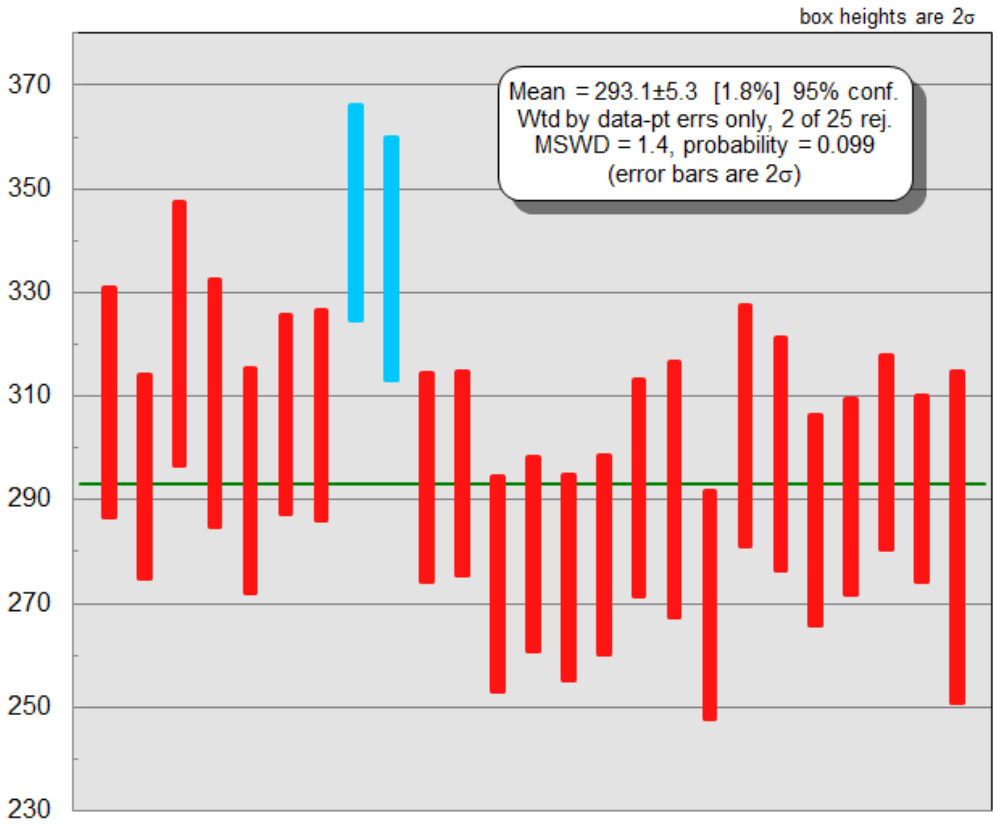

Figure 27: Weighted average of all zircon U-Pb analyses <400 Ma (25 out of 32 analyzed zircons), yielding an age of 293.1 +/- 5.3 Ma.

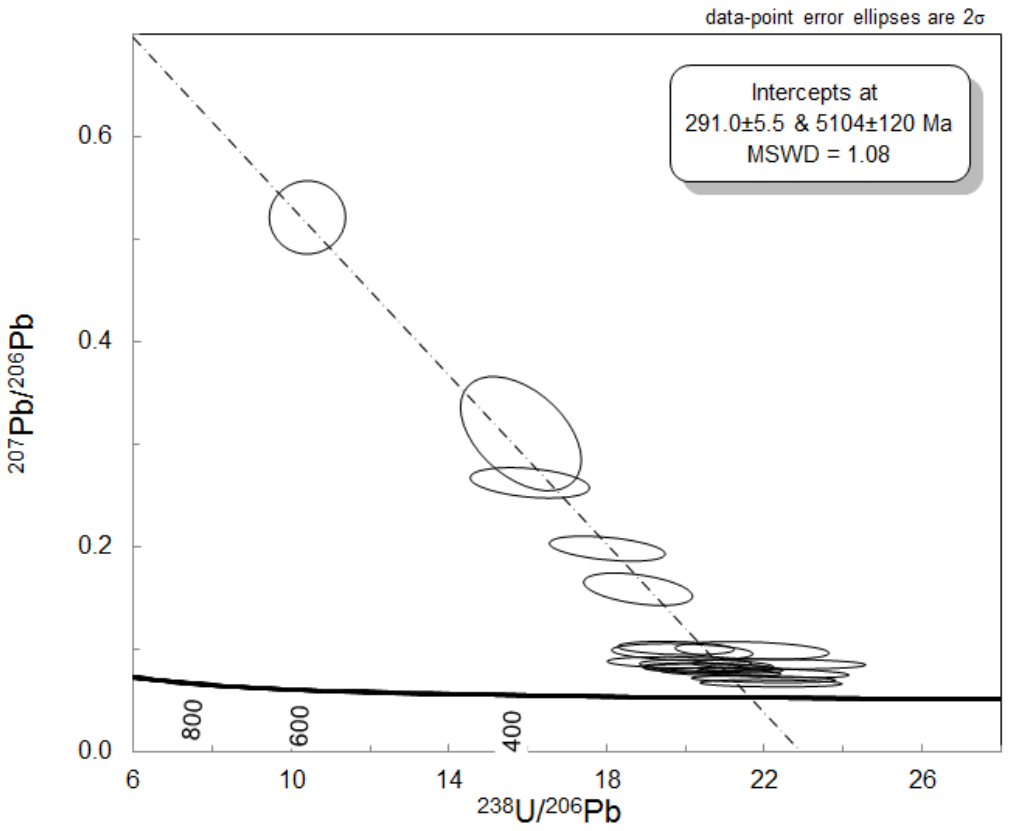

Figure 28: Terra-Wasserburg diagram of more pristine, euhedral zircons of the LICG, yielding intercept age at 291.0 +/- 5.5 Ma which is consistent with the weighted average in Figure 27.

Kowaliga gneisses, but an age of 293.1 ± 5.3 Ma on the LICG is too young to allow the intrusives to be temporally related.

Geochemistry

Six samples of the LICG from the Roanoke East, Alabama, Quadrangle were selected for whole rock and trace element geochemical analyses. All samples occur within the BSZ, with locations indicated in Figures 24 and 25, and Appendix I. Samples weighing approximately 30 grams were sent to Activation Laboratories Ltd. (Ontario, Canada) for commercial analysis using a combination of ICP-MS (inductively coupled plasma mass spectrometry) and INAA (instrumental neutron activation analysis) methods. Results are tabulated in Appendix III. In addition to these analyses, Dr. Karen Tefend (University of West Georgia) provided whole rock analyses of nine samples from the LICG northwest of metro-Atlanta (locations seen in Figure 25) based on XRF (X-ray fluorescence) methods. Results are reported in Appendix IV. From this point forward, samples collected by Dr. Tefend near Atlanta will be referred to as the Georgia LICG. These data were then plotted against previously reported data on the Zana gneiss and Kowaliga gneiss (Stoddard, 1983 and Hawkins, 2013) in order to evaluate any potential relationships between the intrusive bodies.

CIPW normative mineral assemblages were calculated for all samples and plotted on an An-Ab-Or tonalite to granite classification ternary diagram (after Barker, 1979) in Figure 29. All samples of the Alabama LICG plot as true granites, while the Georgia LICG samples follow a more tonalitic to granitic trend. Plotted on an AFM ternary diagram (after Irvine and Baragar, 1971), the LICG follows a calc-alkaline trend along

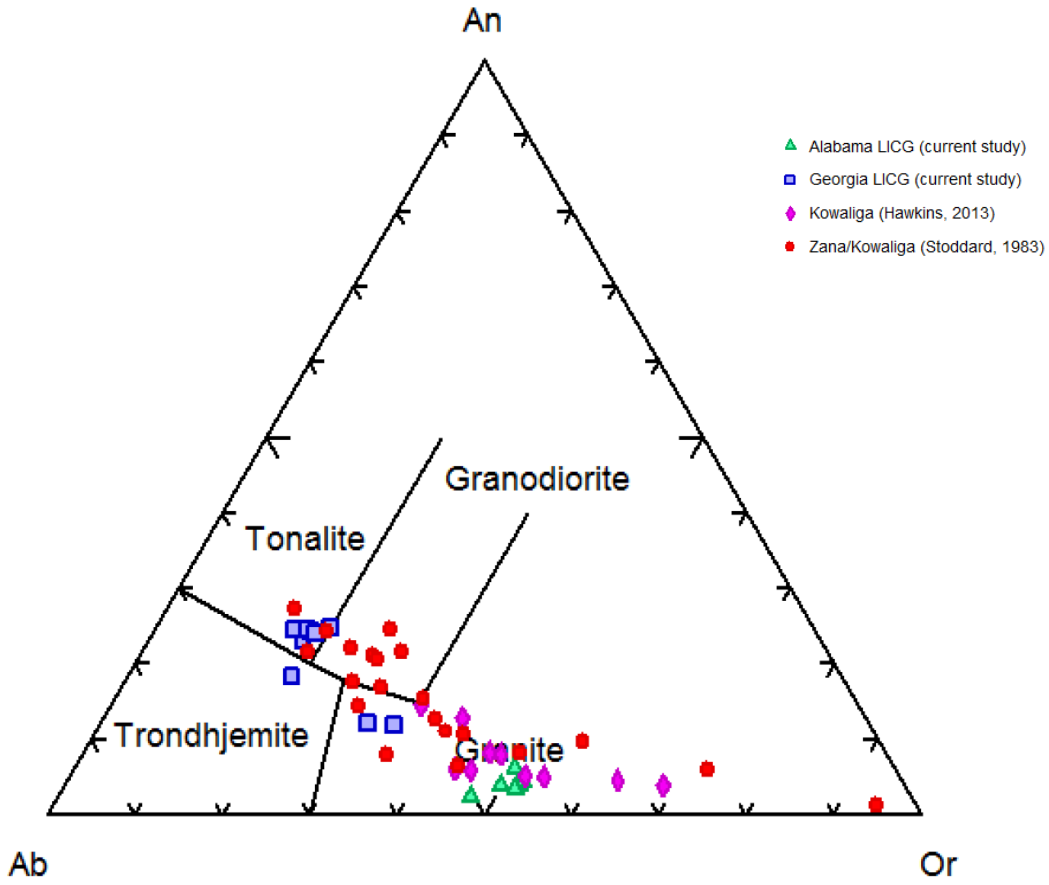

Figure 29: CIPW normative classification for samples of the LICG after Barker (1979).

with the data previously reported on the Zana and Kowaliga gneisses (Figure 30). Harker bivariate plots of eight major oxides (Al_2O_3, CaO, FeO, MgO, Na_2O, TiO_2, K_2O, and P_2O_5) versus silica are reported in Figure 31. In all of these Harker plots, the LICG plots dominantly at the higher end of the silica trend (> 65% SiO_2), particularly those samples from Alabama. The current author interprets that the LICG, at least partially, represents an intrusion that cooled from a highly fractionated melt, resulting in the high silica content that is observed. In all these plots (Figures 29, 30, and 31), the LICG data partly overlaps those previously reported on the Zana and Kowaliga gneisses, however it is important to note that this does not require their correlation if the intrusions are of different ages.

Trace element data on the Alabama LICG and the Kowaliga gneiss (Hawkins, 2013) are plotted using various tectonic discrimination schemes in an effort to constrain a tectonic setting for the LICG. Figure 32 contains Rb-(Yb+Nb) and Rb-(Yb-Ta) plots (after Pearce et al., 1984) showing the LICG predominantly as a within-plate granite and the Kowaliga gneiss as a volcanic-arc granite, with minor overlap between the two. Figure 33 is a Hf-Rb/30-Ta x 3 tectonic discrimination ternary scheme after Harris et al. (1986), and shows the LICG as a volcanic-arc granite with some data lying in the syn-collisional granite field. The Kowaliga gneiss appears to lie within almost every field on the ternary scheme. Due to the conflicting nature of these diagrams (Figures 32 and 33) and the mobile nature of Rb, any insight gained from them based on the currently available data is inconclusive.

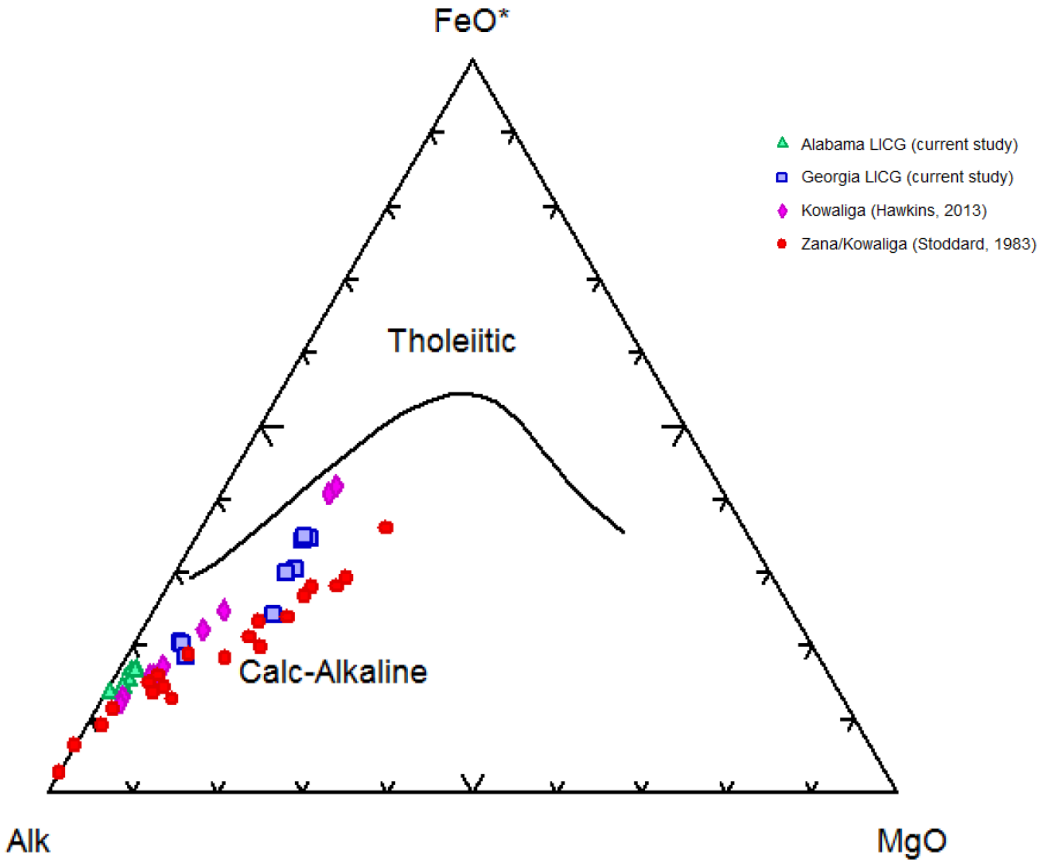

Figure 30: AFM ternary diagram for LICG samples after Irvine and Baragar (1971).

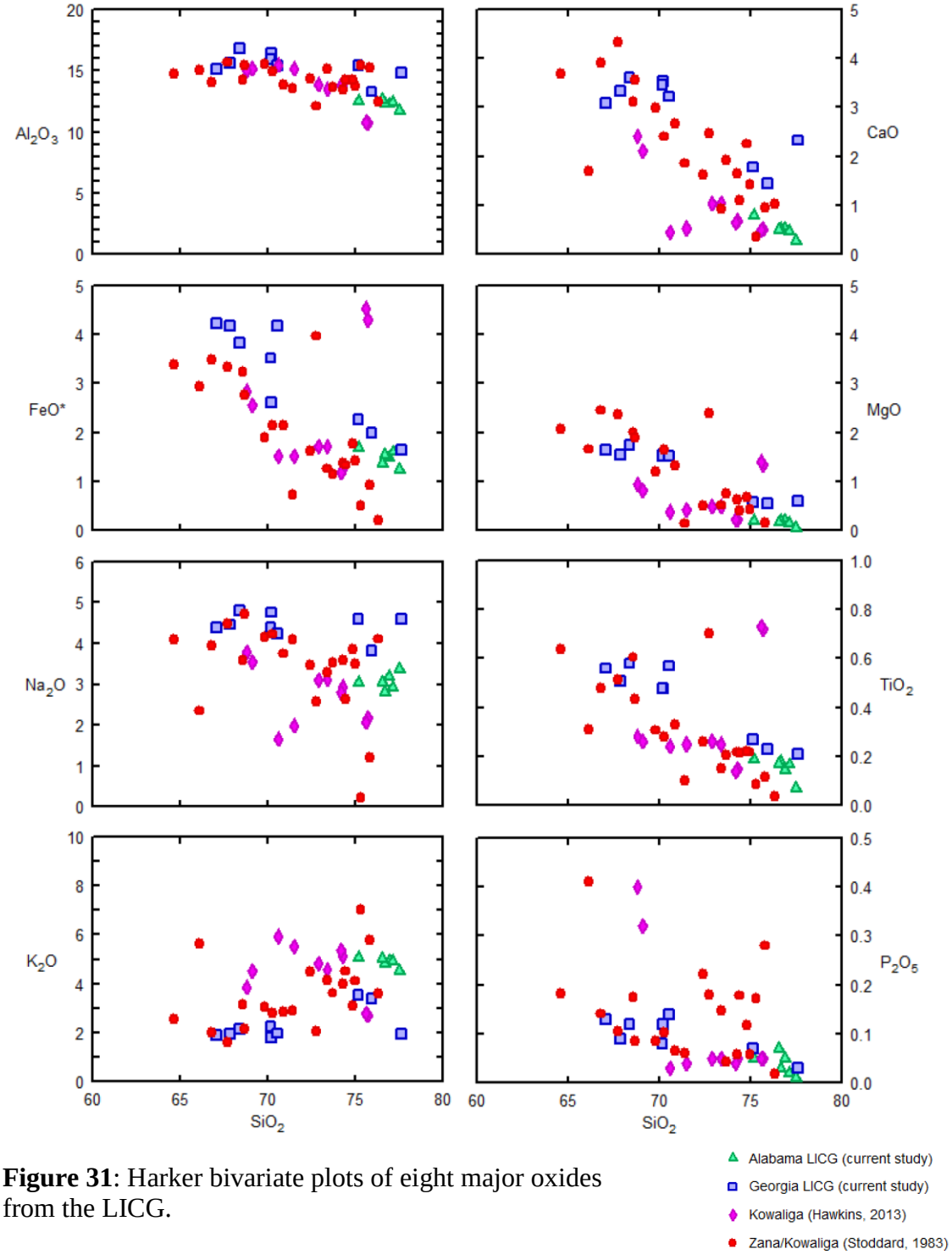

Figure 31: Harker bivariate plots of eight major oxides from the LICG.

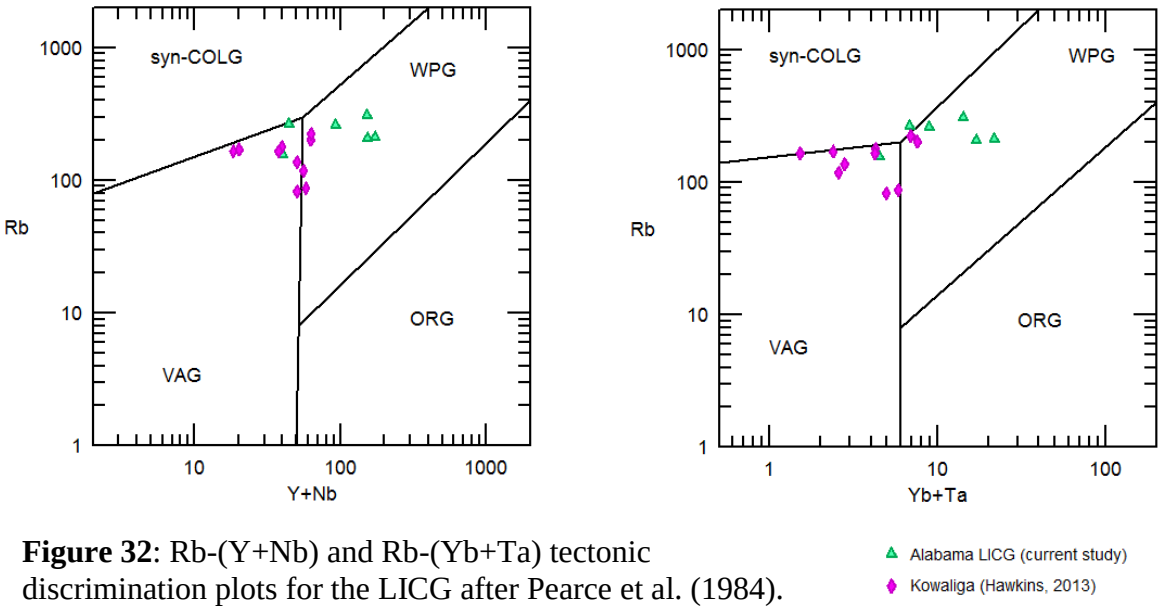

Figure 32: Rb-(Y+Nb) and Rb-(Yb+Ta) tectonic discrimination plots for the LICG after Pearce et al. (1984).

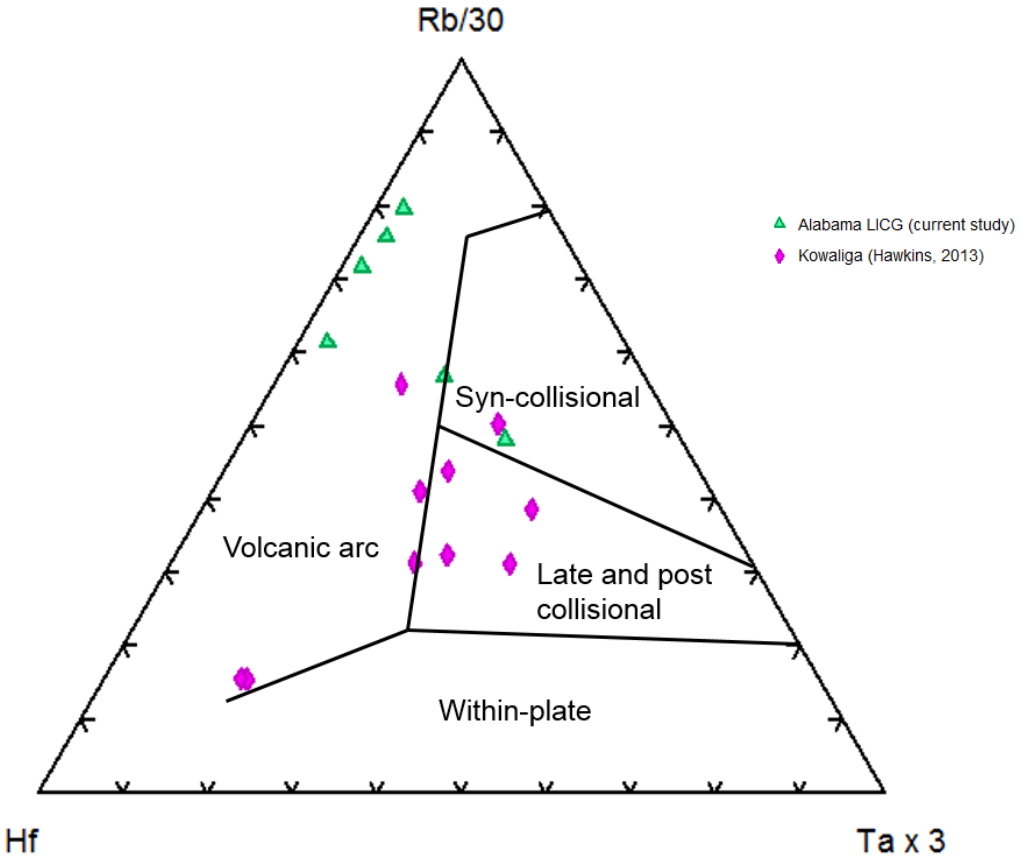

Figure 33: Hf-Rb/30-Ta x 3 tectonic discrimination ternary diagram for LICG and Kowaliga Gneiss (Hawkins, 2013) after Harris et al. (1986).

DISCUSSION

The author originally proposed to explore the hypothetical relationship of the LICG to various Ordovician intrusives in the region (i.e., Zana and Kowaliga gneisses), which may have had implications regarding the relationship of the EBR to the JGG that defines the BSZ. Geochronologic analyses, however, yielded a surprisingly young age of 293.1 +/- 5.3 Ma, making it far too young to be related to the Zana or Kowaliga gneisses. Muscovite cooling ages on rocks encapsulating the LICG (i.e., EBR, JGG, and IP lithologies) yield an early to middle Pennsylvanian (Alleghanian) mean age of ~317.5 Ma, and they are interpreted to record timing of cooling through the ~350 ^{o}C isotherm following the latest metamorphic event (Poole, 2015). While some zircon analyses in this study exhibited low Th/U ratios (<0.1), the current author does not interpret these to be related to metamorphism. Several authors have noted that lower Th/U ratios can be produced in zircons within igneous rocks that cooled from a highly fractionated source (Kirkland et al., 2015), and based on its geochemistry, the LICG is highly fractionated. The current author thus interprets that the ~293 Ma age on the LICG reflects emplacement and igneous crystallization, and not metamorphism. There are other granitic Alleghanian plutons intruding the region with similar ages (Lin, 2015), suggesting that perhaps the LICG was produced from a related magmatic event.

An initial issue of concern was whether the LICG is an orthogneiss (igneous protolith) or a paragneiss (sedimentary protolith). This was questioned given the minor

age population peaks (~450, 600, and 1000 Ma) seen in Figure 26. Igneous structures/features are rarely observed in thin sections of all the LICG samples. Instead, mainly microstructures indicative of solid-state deformation related to movement on the BSZ were observed. The analyzed zircons do exhibit oscillatory zoning however, which is characteristic of magmatic zircons. In addition, an intrusive origin for the LICG protolith is further confirmed by discriminant functions calculated for all LICG geochemical analyses, which yield a positive value indicative of an igneous protolith (Shaw, 1972; calculations in Appendix V). Geochemical analyses, particularly those on samples in Alabama, reveal that the LICG is a granite that was cooled from a highly fractionated melt, thus resulting in the occurrence of some lower Th/U ratios. The minor age population peaks in Figure 26, thus, likely reflect xenocrystic components incorporated during the ascent of the fractionated LICG melt through the crust, as crustal components of each of those age ranges are known to host rocks cut by the Brevard shear zone (VanDervoort, 2015).

The ~293 Ma age for magmatic crystallization of the LICG makes it among the youngest granitic intrusions yet dated from the Alabama Piedmont. It falls at the tail end of the latest period of Alleghanian plutonism that spanned a period of time between ~330 and 295 Ma (Lin, 2015). The LICG orthogneiss-sheet parallels the Brevard shear zone for more than 150 km northeastward into the area near Atlanta, Georgia where the more bulbous sigmoidal-shaped and similarly late-Alleghanian-aged Ben Hill and Palmetto granites (Lin, 2015) have been dextrally-dragged into the Brevard zone (Vauchez, 1987). The intense mylonitic fabric and microstructures of the LICG document syn- to late-syn-magmatic crystallization shearing, which places a maximum on the time of right-slip

movement along the Brevard shear zone at ca. 293 Ma. This timing is compatible with movement along the southern Appalachian decollement and the system of Alleghanian dextral shear zones that lace the southernmost parts of the Appalachians (Secor et al., 1986; Steltenpohl, 1988; Steltenpohl et al., 1992, 2013).

CONCLUSIONS

1. The lithologies of the Jacksons Gap Group within the Roanoke East Quadrangle are not easily divided into separate, mappable units as a result of their gradational nature and similarity to adjacent units (i.e., Emuckfaw Group and Waresville Schist). This paucity of distinct mappable units (e.g., orthoquartzites, metaconglomerates, and graphite quartzites), also reported from the Wadley South Quadrangle (VanDervoort, 2015), contrasts sharply with observations further to the southwest and is perhaps a result of along-strike structural and/or stratigraphic variations (e.g., Sterling, 2006; Hawkins, 2013; Abrahams, 2014; and Poole, 2015). Thus, within the Roanoke East Quadrangle, lithologies of the Jacksons Gap Group are divided into two main lithofacies types: a structurally lower section defined mostly by garnetiferous-graphitic-quartz-biotite schists and phyllites interlayered with micaceous quartzites, and an upper section of variably graphitic, garnetiferous-sericite-chlorite schists and phyllites, with no interlayered quartzites. These lithologies are intruded by the Long Island Creek Gneiss.

2. The metapelitic lithologies of the Jacksons Gap Group within the Roanoke East Quadrangle are not easily distinguishable from some lithologies of the immediately adjacent units of the Emuckfaw Group and the structurally lower parts of the Waresville Schist. Particularly problematic are the garnetiferous-

graphitic-quartz-biotite schists at the structural bottom of the Jacksons Gap Group and the variably graphitic-garnetiferous-sericite-chlorite schists within the upper Jacksons Gap Group. Combined with the current author's lack of finding cataclasites marking faults bounding the Brevard shear zone, placing the upper and lower contacts of the Brevard shear zone proved to be a difficult task.

3. The current author defines the upper limit of the Emuckfaw Group within the Roanoke East Quadrangle based on the lack of metagraywackes and rare, thin amphibolites. The lower limit of the Waresville Schist is based on the occurrence of amphibolites, interpreting them to be part of the metavolcanics of the Dadeville Complex. This contrasts with the work done by Kath (personal communication to M.G. Steltenpohl, 2016), where these same amphibolites are placed within the Brevard shear zone between the Abanda and Katy Creek faults, making their Brevard shear zone significantly thicker than the current author suggests.

4. The Long Island Creek Gneiss does not cross over the boundaries of the Brevard shear zone within the Roanoke East quadrangle, but appears to do so in areas outside of the current study area based on previous maps (Alabama and Georgia state geologic maps; i.e., Osborne et al., 1988 and Pickering, 1976, respectively). The current author suggests that the Long Island Creek Gneiss intrudes the Jacksons Gap Group lithologies, and is stretched/sheared along the Brevard zone shears, particularly the Katy Creek fault within the Roanoke East Quadrangle.

5. Dadeville Complex lithologic units and their associated early-metamorphic fabrics (Taconian?) are truncated along the syn- to late-D_1 Katy Creek fault, which later was overprinted by D_2 and D_3 retrograde dextral shearing. An inverted metamorphic gradient appears to correspond to the Katy Creek fault, which may have been formed as a result of down-heating that occurred during the emplacement of the hot Dadeville Complex on top of the cooler Jacksons Gap Group. The amalgamation of the Jacksons Gap Group and the Dadeville Complex occurred no earlier than the Acadian, as evidence for Taconic metamorphism in the hanging wall (VanDervoort et al., 2015) is lacking in the footwall units.

6. The age of Rock Mills Granite Gneiss remains to be constrained. The current author suggests, however, that it must be younger than the 466 Ma Waresville Schist that it intrudes (VanDervoort et al., 2015).

7. The Long Island Creek Gneiss was emplaced at 293.1 +/- 5.3 Ma representing a later, more highly fractionated melt that cooled at the end of the period of Alleghanian plutonism which spanned a period of time between ~330 and 295 Ma (Lin, 2015). Combined with field and microstructural observations, the ~293 Ma date places a maximum on the timing of dextral movement along the Brevard shear zone.

REFERENCES

Abbott, R.N., and Raymond, L.A., 1984, The Ashe Metamorphic Suite, northwest North Carolina: Metamorphism and observations of geologic history: American Journal of Science, v. 284, p. 350-375, doi: 10.2475/ajs.284.4-5.350.

Abbott, R.N., and Raymond, L.A., 1997, Petrology of pelitic and mafic rocks in the Ashe and Alligator Back metamorphic suites, northeast of the Grandfather Mountain Window, *in* Stewart, K.G., Adams, M.G., and Trupe, C.H., eds., Paleozoic Structure, Metamorphism, and Tectonics of the Blue Ridge of Western North Carolina: Durham, Carolina Geological Society, v. 1997, p. 87-101.

Abrahams, J.B., 2014, Geology of the Dadeville Quadrangle and the Tallassee synform in characterizing the Dog River window: unpublished M.S. thesis, Auburn University, Auburn, Alabama, 126 p.

Absher, B.S., and McSween, H.Y., 1986, Winding Stair Gap granulites: The thermal peak of Paleozoic metamorphism: Geological Society of America Centennial Field Guide – Southeastern Section, p. 257-260.

Adams, G.I., 1926, The crystalline rocks *in* Adams, G.I., Butts, D., Stephenson, L.W., and Cooke, C.W., eds., Geology of Alabama: Alabama Geological Survey Special Report 14, p. 40-223.

Adams, G.I., 1930, Gold deposits of Alabama, and occurrences of copper, pyrite, arsenic and tin: Alabama Geological Survey Bulletin 40, 91 p.

Adams, M.G., Stewart, K.G., Trupe, C.H., and Willard, R.A., 1995, Tectonic significance of high-pressure metamorphic rocks and dextral strike slip faulting in the southern Appalachians, *in* Hibbard, J.P., van Staal, C.R., and Cawood, P., eds., Current Perspectives in the Appalachian-Caledonian Orogen: Geological Association of Canada Special Paper 41, p. 21-42.

Allison, D.T., 1992, Structural evolution and metamorphic petrogenesis of a metasediment and metaigneous complex, Coosa County, Alabama: unpublished Ph.D. dissertation, Florida State University, Tallahassee, Florida, 378 p.

Barineau, C.I., and Tull, J.F., 2012, The Talladega and Ashland-Wedowee-Emuckfaw belts of Alabama: Geological overview, *in* Barineau, C.I., and Tull, J.F., eds., The Talladega Slate Belt and the eastern Blue Ridge: Laurentian plate passive margin to back-arc basin tectonics in the southern Appalachian orogen: Alabama Geological Society 49th Annual Field Trip Guidebook, p. 27-37.

Barineau, C.I., Tull, J.F., Holm-Denoma, C.S., 2015, A Laurentian margin back-arc: The Ordovician Wedowee-Emuckfaw-Dahlonega basin, *in* Holmes, A.E., ed., Diverse Excursions in the Southeast: Paleozoic to Present: Geological Society of America Field Guide 39, p. 21-78.

Barker, F., 1979, Trondhjemite: Definition, environment, and hypotheses of origin: Trondhjemites, dacites, and related rocks, p. 1-12.

Bentley, R.D., and Neathery, T.L, 1970, Geology of the Brevard shear zone and related rocks of the Inner Piedmont of Alabama: Alabama Geological Society Field Trip Guidebook, n. 8, 119 p.

Bream, B.R., 2002, The southern Appalachian Inner Piedmont: New perspectives based on recent detailed geologic mapping, Nd isotopic evidence and zircon geochronology, *in* Hatcher, R.D., and Bream, B.R., eds., Inner Piedmont Geology in the South Mountains-Blue Ridge Foothills and the southwestern Brushy Mountains, central western North Carolina: North Carolina Geological Survey, Carolina Geological Society Annual Field Trip Guidebook, p. 45-63.

Bream, B.R., 2003, Tectonic implications of geochronology and geochemistry of para- and orthogneisses from the southern Appalachian crystalline core: unpublished Ph.D. dissertation, University of Tennessee, Knoxville, Tennessee, 296 p.

Carrigan, C.W., Bream, B., Miller, C.F., and Hatcher, R.D., Jr., 2001, Ion microprobe analyses of zircon rims from the eastern Blue Ridge and Inner Piedmont, NC-SC-GA: Implications for the timing of Paleozoic metamorphism in the southern Appalachians: Geological Society of America Abstracts with Programs, v. 33, p. 7.

Crawford, T.J., and Kath, R.L., 2015, Geologic Map of the Brevard zone from central Georgia to eastern Alabama: Geological Society of America Abstracts with Programs, v. 47, n. 2, p. 31.

Crawford, T.J., Higgins, M.W., Crawford, R.F., Atkins, R.L., Medlin, J.H., and Stern, T.W., 1999, Revision of stratigraphic nomenclature in the Atlanta, Athens, and Cartersville 30’ x 60’ quadrangles, Georgia, Environmental Protection Division, Georgia Department of Natural Resources, Bulletin 130, p. 38.

Cook, F.A., Albuagh, D.S., Brown, L.D., Kaufman, S., Oliver, J.E., and Hatcher, R.D., Jr., 1979, Thin-skinned tectonics in the crystalline southern Appalachians; COCORP seismic-reflection profiling of the Blue Ridge and Piedmont: Geology, v. 7, p. 563-567.

Cyphers, S.R., and Hatcher, R.D., Jr., 2006, The Chattahoochee-Holland mountain fault: A terrane boundary in the Blue Ridge of western North Carolina: Geological Society of America Abstracts with Programs, v. 38, n. 3, p. 66.

Dennis, A.J., and Wright, J.E., 1997, Middle and late Paleozoic monazite U-Pb ages, Inner Piedmont, South Carolina: Geological Society of America Abstracts with Programs, v. 29, n. 3, p. 12.

Drummond, M. S., 1986, Igneous, metamorphic, and structural history of the Alabama Tin Belt, Coosa County, Alabama: unpublished Ph.D. dissertation, Florida State University, Tallahassee, Florida, 411 p.

Drummond, M.S., Neilson, M.J., Allison, D.T., and Tull, J.F., 1997, Igneous petrogenesis and tectonic setting of granitic rocks from the eastern Blue Ridge and Inner Piedmont, Alabama Appalachians, *in* Sinha, A.K., et al., eds., The nature of magmatism in the Appalachian orogen: Geological Society of America Memoir 191, p. 147-164.

Ernst, W.G., 1973, Interpretative synthesis of metamorphism in the Alps: Geological Society of America Bulletin, v. 84, p. 2053-2078.

Farris, D.W., Tull, J.F., Mueller, P.A., Davis, B.L., and Thomas, R., 2015, The Dadeville Complex of eastern Alabama and western Georgia: Implications for the "missing" Taconic arc in the southern Appalachians, Geological Society of America Abstracts with Programs, v. 47, n. 7, p. 863.

Garihan, J.M., and Ranson, W.A., 1992, Structure of the Mesozoic Marietta-Tryon graben, South Carolina and adjacent North Carolina, in Bartholomew, M.J., et al., eds., Basement tectonics 8: Characterization of ancient and Mesozoic continental margins—Proceedings of the 8th International Conference on Basement Tectonics, Butte, Montana, 1988: Dordrecht, Netherlands, Kluwer Academic Publishers, p. 539–555.

Garihan, J.M., Preddy, M.S., and Ranson, W.A., 1993, Summary of mid-Mesozoic brittle faulting in the Inner Piedmont and nearby Charlotte belt of the Carolinas, in Hatcher, R.D., Jr., and Davis, T., eds., Studies of Inner Piedmont geology with a focus on the Columbus Promontory: Carolina Geological Society Field Trip Guidebook, p. 55–66.

Goldberg, S.A., and Steltenpohl, M.G., 1990, Timing and characteristics of Paleozoic deformation and metamorphism in the Alabama Inner Piedmont: American Journal of Science, v. 290, p. 1169-1200.

Grimes, J.E., 1993, Geology of the Piedmont rocks between the Dadeville Complex and the Pine Mountain Window in parts of Lee, Macon, and Tallapoosa Counties, Alabama: unpublished M.S. thesis, Auburn University, Auburn, Alabama, 129 p.

Grimes, J.E., and Steltenpohl, M.G., 1993, Geology of the crystalline rocks along the fall line, on the Carrville, Notasulga, and Loachapoka quadrangles, Alabama, *in* Steltenpohl, M.G., and Salpas, P.A., eds., Geology of the southernmost exposed Appalachian Piedmont rocks along the Alabama fall line: Geological Society of America, Southeastern section 42nd Annual Meeting Field Trip Guidebook, p. 67-94.

Guthrie, G.M., and Dean, L.S., 1989, Geology of the New Site 7.5-minute Quadrangle, Tallapoosa and Clay counties, Alabama: Alabama Geological Survey Quadrangle Map 9, 41 p.

Hames, W.E., Tull, J.F., Barbeau, D.L., Jr., McDonald, W.M., and Steltenpohl, M.G., 2007, Laser $^{40}Ar/^{39}Ar$ ages of muscovite and evidence for Mississippian (Visean) deformation near the thrust front of the southwestern Blue Ridge province: Geological Society of America Abstracts with Programs, v. 39, n. 2, p. 78.

Harris, N.B.W., Pearce, J.A., and Tindle, A.G., 1986, Geochemical characteristics of collision-zone magmatism: Collision tectonics, Special Publication Geological Society, p. 67-81.

Harstad, R.P., and Barineau, C.I., 2014, Kinematic and age constraints on the Alexander City fault, eastern Blue Ridge, Alabama, Geological Society of America Abstracts with Programs, v. 45, n. 6, p. 504.

Hatcher, R.D., Jr., 1989, Tectonic synthesis of the U.S. Appalachians, Chapter 14, *in* Hatcher R.D., Jr., Thomas, W.A., and Viele, G.W., eds., The Appalachian-Ouachita Orogen in the United States: Geology of North America, Geological Society of America, v. F-2, p. 511-535.

Hatcher, R.D., Jr, 2005, Southern and central Appalachians, *in* Selley R.C., Cocks, L.R.M., and Plimer, I.R. eds., Encyclopedia of Geology, Elsevier Academic Press, Amsterdam, p. 72-81.

Hawkins, J.F., 2013, Geology, petrology, and geochronology of rocks in the Our Town, Alabama Quadrangle: unpublished M.S. thesis, Auburn University, Auburn, Alabama, 118 p.

Higgins, M.W., Atkins, R.L., Crawford, T.J., Crawford, R.E., Brooks R., and Cook, R.B., 1988, The structure, stratigraphy, tectonostratigraphy and evolution of the southernmost part of the Appalachian orogen: U.S. Geological Survey Professional Paper 1475, 173 p.

Hirth, G., and Tullis, J., 1994, The nature of the brittle to plastic transition in quartz aggregates: Journal of Geophysical Research, v. 99, p. 11731–11748, doi:10.1029/93JB02873.

Holdaway, M.J., 1971, Stability of andalusite and the aluminosilicate phase diagram: American Journal of Science, v. 271, p. 97-131.

Irvine, T.N., and Baragar, W.R.A., 1971, A guide to the chemical classification of the common volcanic rocks: Canadian Journal of Earth Sciences, v. 8, p. 523-548.

Johnson, M.J., 1988, Geology of the gold occurrences near Jacksons Gap, Tallapoosa County, Alabama: unpublished M.S. thesis, Auburn University, Auburn, Alabama, p. 156.

Keefer, W.D., 1992, Geology of the Tallassee synform hinge zone and its relationship to the Brevard shear zone, Tallapoosa and Elmore Counties: unpublished M.S. thesis, Auburn University, Auburn, Alabama, 195 p.

Kirkland, C.L., Smithies, R.H., Taylor, R.J.M., Evans, N., and McDonald, B., 2015, Zircon Th/U ratios in magmatic environs: Lithos, v. 2-12-215, p. 397-414

Kohn, M.J., 2001, Timing of arc accretion in the southern Appalachians: Perspectives from the Laurentian margin: Geological Society of America Abstracts with Programs, v. 33, n. 6, p. 262.

Lin, Q., 2015, Spatial-temporal distribution of the Alleghanian magmatism in the southern Appalachians: Implication of the assembly of supercontinent Pangea: unpublished M.S. thesis, University of Florida, Gainesville, Florida, 160 p.

Ludwig, K.R., 2012, Isoplot 3.75: A Geochronological Toolkit for Microsoft Excel: Berkeley Geochronology Center Special Publication 5, 75 p.

McClellan, E.A., Steltenpohl, M.G., Thomas, C., and Miller, C., 2007, Isotopic age constraints and metamorphic history of the Talladega belt: New evidence of timing of arc magmatism and arc emplacement along the southern Laurentian margin: The Journal of Geology, v. 115, p. 541-561.

McCullars, J.M., 2001, Geology and trace-element geochemistry of the Brevard zone near Martin Lake, Tallapoosa County, Alabama: unpublished M.S. thesis, Auburn University, Auburn, Alabama, 74 p.

McDonald, W.M., Hames, W.E., Marzen, L.J., and Steltenpohl, M.G., 2007, A GIS database for 40Ar/39Ar data of the southwestern Blue Ridge province: Geological Society of America Abstracts with Programs, v. 39, n. 2, p. 81. 44

Medlin, J.H., and Crawford, T.J., 1973, Stratigraphy and structure along the Brevard fault zone in western Georgia and Alabama: American Journal of Science, v. 273-A, p. 89-104.

Merschat, A.J., Hatcher, R.D., Jr., Bream, B.R., Miller, C.F., Byars, H.E., Gatewood, M.P., and Wooden, J.L., 2010, Detrital zircon geochronology and provenance of southern Appalachian Blue Ridge and Inner Piedmont crystalline terranes, *in* Tollo, R.P., Bartholomew, M.J., Hibbard, J.P., and Karabinos, P.M., eds., From Rodinia to Pangea: The Lithotectonic Record of the Appalachian Region: Geological Society of America Memoir, v. 206, p. 661-699.

Muangnoicharoen, N., 1975, The geology and structure of a portion of the northern piedmont, east-central Alabama: unpublished M.S. thesis, University of Alabama, Tuscaloosa, Alabama, p. 72.

Neathery, T.L., and Reynolds, J.W., 1975, Geology of the Lineville East, Ofelia, Wadley North and Mellow Valley Quadrangles, Alabama: Geological Survey of Alabama Bulletin, v. 109, 120 p.

Osborne, W.E., Szabo, M.W., Neathery, T.L., and Copeland, C.W., Jr., compilers, 1988, Geologic map of Alabama, northeast sheet: Alabama Geological Survey Special Map 220, scale 1:250,000.

Pardee, J.T., and Park, C.F., Jr., 1948, Gold deposits of the southern Piedmont: U.S. Geological Survey Professional Paper 213, 156 p.

Park, C.F., Jr., 1935, Hog mountain gold district, Alabama: American Institute of Mining and Metallurgical Engineers Transactions, Mining Geology, v. 115, p. 209-228.

Passchier, C.W., and Trouw, R.A.J., 2005, Microtectonics: 2nd edition, Springer-Verlag, Heidelberg, Germany, 366 p.

Pearce, J.A., Harris, N.B.W., and Tindle, A.G., 1984, Trace element discrimination diagrams for the tectonic interpretation of granitic rocks: Journal of Petrology, v. 25, p. 956-983.

Phillips, W. B., 1892, a preliminary report on a part of the lower gold belt of Alabama in the counties of Chilton, Coosa, and Tallapoosa: Alabama Geological Survey Bulletin 3, 97 p.

Pickering, S., 1976, ed., Geologic Map of Georgia: Georgia Geologic Survey, Atlanta, Georgia, scale 1:500,000.

Poole, J.D., 2015, Geology of the Jacksons Gap, Alabama, Quadrangle and structural implications for the Brevard shear zone: unpublished M.S. thesis, Auburn University, Auburn, Alabama, 153 p.

Raymond, D.E., Osborne, W.E., Copeland, C.W., and Neathery, T.L., 1988, Alabama Stratigraphy: Geological Survey of Alabama, Tuscaloosa, 97 p.

Raymond, L. A., Yurkovich, S. P. and McKinney, M., 1989. Block-in-matrix structures in the North Carolina Blue Ridge belt and their significance for the tectonic history of the southern Appalachian orogen. Geological Society of America Special Paper, p. 195-215.

Reed, A.S., 1994, Geology of the western portion of the Dadeville 7.5' Quadrangle, Tallapoosa County, Alabama: unpublished M.S. thesis, Auburn University, Auburn, Alabama, 108 p.

Reynolds, A.L., and Steltenpohl, M.G., 2009, Geologic map of the 1:24,000 Red Hill, Alabama, U.S.G.S. Topographic Quadrangle: Alabama Geological Survey Open-File Special Map.

Roop-Eckart, K.J., and Barineau, C.I., 2015, Strain analysis across the margins of the Elkahatchee and Coley Creek plutons, Alabama eastern Blue Ridge: Implications for the Alexander City Fault: Geological Society of America Abstracts with Programs, v. 47, n. 7, p. 537.

Russell, G.S., 1978, U-Pb, Rb-Sr., and K-Ar geochronology of the Alabama Piedmont: unpublished Ph.D. dissertation, Florida State University, Tallahassee, Florida, 198 p.

Sagul, D.A., 2016, Constraining the age and petrogenesis of the Zana and Kowaliga Gneisses, eastern Blue Ridge, Alabama: unpublished M.S. thesis, University of Florida, Gainesville, Florida, 150 p.

Scholz, C.H., 1988, The brittle-plastic transition and depth of seismic faulting: Geologische Rundschau, v. 77, p. 319–328, doi:10.1007/BF01848693.

Schwartz, J.J., Johnson, K., Ingram, S., 2011, U-Pb zircon geochronology of Neoacadian and Early Alleghenian plutonic rocks in the Alabama Eastern Blue Ridge, Southern Appalachian Mountains, Geological Society of America Abstracts with Programs, v. 43, n. 1, p. 62.

Secor, D.T., Snoke, A.W., and Dallmeyer, R.D., 1986, Character of the Alleghanian orogeny in the southern Appalachians: Part III Regional tectonic relations: Geological Society of America Bulletin, v. 97, p. 1345-1353.

Shaw, D.M., 1972, The origin of the Apsley Gneiss, Ontario: Canadian Journal of Earth Sciences, v. 9, p. 18-35.

Simpson, C., and Schmid, S., 1983, An evaluation of criteria to deduce the sense of movement in sheared rocks: Geological Society of America Bulletin, v. 94, p. 1281–1288, doi:10.1130/0016-7606(1983)94<1281:AEOCTD>2.0.CO;2.

Singleton, R.F., and Steltenpohl, M.G., 2014, Geology of the 1:24,000 Buttston, Alabama, 7.5-Minute Quadrangle, Tallapoosa County, Alabama: Alabama Geological Survey Open-File Report, 30 p.

Sinha, A.K., and Higgins, M.W., 1987, Localization of melts along structural discontinuities in the southern Appalachians: consequences of overthrusting and decompressional melting, Geological Society of America Abstracts with Programs, v. 19, n. 7, p. 847.

Stahr, D. W., III, Hatcher, R.D., Jr., Miller, C.F., and Wooden, J.L., 2006, Alleghanian deformation in the Georgia and North Carolina eastern Blue Ridge: Insights from pluton ages and fabrics: Geological Society of America Abstracts with Programs, v. 38, n. 3, p. 20.

Steltenpohl, M.G., 1988, Kinematics of the Towaliga, Bartletts Ferry, and Goat Rock fault zones: The late Paleozoic dextral shear system in the southernmost Appalachians: Geology, v. 16, p. 852-855.

Steltenpohl, M.G., 2005, An introduction to the terranes of the southernmost Appalachians of Alabama and Georgia, *in* Steltenpohl, M.G., ed., Southernmost Appalachian terranes, Alabama and Georgia: Southeastern Section of the Geological Society of America Field Trip Guidebook, p. 1-18.

Steltenpohl, M.G., 2014, Geology of the 1:24,000 Roanoke East, Alabama, Quadrangle: Unpublished EDMAP proposal summary sheet, 16 p.

Steltenpohl, M.G., and Kunk, M.J., 1993, 40Ar/39Ar thermochronology and Alleghanian development of the southernmost Appalachian Piedmont, Alabama and southwest Georgia: Geological Society of America Bulletin, v. 105, p. 819-833.

Steltenpohl, M.G., and Moore, W.B., 1988, Metamorphism in the Alabama Piedmont: Alabama Geological Survey Circular 138, 29 p.

Steltenpohl, M.G., Cook, R.B., Grimes, J.E., Keefer, W.D., Heatherington, A., and Mueller, P., 2005, Geology of the Brevard zone in the hinge of the Tallassee synform, Alabama Fall Line: Implications for southernmost Appalachian tectonostratigraphy, *in* Steltenpohl, M.G., ed., New Perspectives on Southernmost Appalachian terranes, Alabama and Georgia: Geological Society of Alabama 43rd Annual Trip Guidebook, Alabama Geological Society, Tuscaloosa, p. 125-148.

Steltenpohl, M.G., Goldberg, S.A., Hanley, T.B., and Kunk, M.J., 1992, Evidence for Alleghanian development of the Goat Rock fault zone, Alabama and southwest Georgia: Temporal compatibility with the master decollement: Geology, v. 20, p. 845-848.

Steltenpohl, M.G., Neilson, M.J., Bittner, E.I., Colberg, M.R., and Cook, R.B., 1990, Geology of the Alabama Inner Piedmont terrane: Geological Survey of Alabama Bulletin 139, 80 p.

Steltenpohl, M.G., Schwartz, J.J., and Miller, B.V., 2013, Late- to post-Appalachian strain partitioning and extension in the Blue Ridge of Alabama and Georgia: Geosphere, v. 9, n. 3, p. 647-666.

Sterling, J.W., 2006, Geology of the southernmost exposures of the Brevard zone in the Red Hill Quadrangle, Alabama: unpublished M.S. thesis, Auburn University, Auburn, Alabama, 118 p.

Sterling, J.W., Steltenpohl, M.G., and Cook, R.B., 2005, Petrology and geochemistry of igneous rocks in the southernmost Brevard zone of Alabama and their implications for southern Appalachian tectonic evolution, *in* Steltenpohl, M.G., New perspectives on Southernmost Appalachian terranes, Alabama and Georgia: Alabama Geological Society 42nd Annual Field Trip Guidebook, p. 96-124.

Stoddard, P.V., 1983, A petrographic and geochemical analysis of the Zana Granite and Kowaliga Augen Gneiss: Northern Piedmont, Alabama: unpublished M.S. thesis, Memphis State University, Memphis, Tennessee, 74 p.

Stowell, H.H., Lesher, C.M., Green, N.L., and Sha, P., 1996, Metamorphism and gold mineralization in the Blue Ridge southernmost Appalachians: Economic Geology, v. 91, p. 1115-1144.

Tull, J.F., Barineau, C.I., and Holm-Denoma, C.S., 2012, Characteristics, Extent, and Tectonic Significance of the Middle Ordovician Back-Arc Basin in the Southern Appalachian Blue Ridge, *in* Barineau, C.I., and Tull, J.F., eds., The Talladega Slate Belt and the eastern Blue Ridge: Laurentian plate passive margin to back-arc basin tectonics in the southern Appalachian orogen: Alabama Geological Society Annual Field Trip Guidebook, p. 12-26.

Tull, J.F., Holm-Denoma, C.S., and Barineau, C.I., 2014, Early to Middle Ordovician back-arc basin in the southern Appalachian Blue Ridge: Characteristics, extent, and tectonic significance: Geological Society of America Bulletin, v. 126, p. 990-1015.

Tullis, J.A., 1983, Deformation of feldspars, in Ribbe, P.H., ed., Feldspar mineralogy: Mineralogical Society of America Short Course Notes, v. 2, p. 297–323.

Tullis, J., 2002, Deformation of granitic rocks: Experimental studies and natural examples, in Karato, S.-I., and Wenk, H.-R., eds., Plastic deformation of minerals and rocks: Mineralogical Society of America Reviews in Mineralogy and Geochemistry Volume 51, p. 97–120.

Tullis, J., and Yund, R.A., 1992, The brittle-ductile transition in feldspar aggregates: An experimental study, in Evans, B., and Wong, T.F., eds., Fault mechanics and transport properties of rocks: New York, Academic Press, p. 89–118.

Tuomey, M., 1858, Second biennial report on the geology of Alabama: Alabama Geological Survey Biennial report 2, 292 p.

VanDervoort, D.S., 2015, Geology of the Wadley South Quadrangle and geochronology of the Dadeville Complex, southernmost Appalachians of east Alabama: unpublished M.S. thesis, Auburn University, Auburn, Alabama, 127 p.

VanDervoort, D.S., and Steltenpohl, M.G., 2015, Geology of the 1:24,000 Wadley South, Alabama, Quadrangle: Geological Survey of Alabama Open-File Report, 34 p.

VanDervoort, D.S., Ma, C., Steltenpohl, M.G., and Schwartz, J.J., 2017, The early Paleozoic (Taconic) Dadeville arc complex, southernmost Appalachians of Alabama and Georgia: Implications for the crustal growth of eastern North America: Geological Society of America Abstracts with Programs, v. 49, n. 3, doi: 10.1130/abs/2017SE-290867.

VanDervoort, D.S., Steltenpohl, M.G., and Schwartz, J.J., 2015, U-Pb ages from the Dadeville Complex, southernmost Appalachians, eastern Alabama: an accreted Taconic arc, Geological Society of America Abstracts with Programs, v. 47, n. 7, p. 159.

Vauchez, A., 1987, Brevard fault zone, southern Appalachians: A medium-angle, dextral, Alleghanian shear zone: Geology, v. 15, p. 669-672.

White, T.W., 2007, Geology of the 1:24,000 Tallassee, Alabama, Quadrangle, and its implications for southern Appalachian tectonics: unpublished M.S. thesis, Auburn University, Auburn, Alabama, 74 p.

Wielchowsky, C.C., 1983, The geology of the Brevard zone and adjacent terranes in Alabama: unpublished Ph.D. dissertation, Rice University, Houston, Texas, 237 p.

APPENDIX

Appendix I: Sample list of Long Island Creek Gneiss sources

Appendix II: LA-SF-ICP-MS analyses of zircons

Appendix III: Geochemical analyses of the Alabama LICG

Appendix IV: Geochemical analyses of the Georgia LICG

Appendix V: Discriminatory analysis of the LICG after Shaw (1972)

Appendix I. Sample list of Long Island Creek Gneiss sources

Sample ID	Location (WGS 84)	AL/GA	Collector*	Geochemistry	Geochronology
RRE-15	33.1993˚N, -85.3418˚W	AL	RPH	x	x
RRE-31	33.2156˚N, -85.3099˚W	AL	RPH	x	
RRE-32B	33.2156˚N, -85.3089˚W	AL	RPH	x	
RRE-110	33.2218˚N, -85.2918˚W	AL	RPH	x	
RRE-149	33.1856˚N, -85.3590˚W	AL	RPH	x	
FRE-18	33.1899˚N, -85.3499˚W	AL	RPH	x	
1	N/A	GA	KST	x	
2	N/A	GA	KST	x	
3	N/A	GA	KST	x	
4	N/A	GA	KST	x	
5	N/A	GA	KST	x	
6	N/A	GA	KST	x	

* RPH is the author of this thesis and KST is Dr. Karen Tefend (University of West Georgia).

Appendix II. LA-SF-ICP-MS analyses of zircons

Anhedral Zircons				Radiogenic Ratios					Ages (Ma)			
Sample (n=15)	U (ppm)	Th (ppm)	$^{232}Th/^{238}U$	$^{238}U/^{206}Pb$	2 σ (%) err	$^{207}Pb/^{206}Pb$	2 σ (%) err	$^{207}Pb/^{206}Pb$	2 σ abs err	$^{206}Pb/^{238}U$	2 σ abs err
Anhe_1_6_1	217	7.38	0.136	19.685	7.09%	0.079	4.18%	**1171**	**78**	***309.21***	***21.63***
Anhe_1_6_2	194	7.40	0.135	20.661	6.61%	0.079	4.93%	**1169**	**90**	***294.78***	***19.28***
Anhe_1_6_3	174	7.69	0.130	18.051	7.76%	0.113	7.26%	**1790**	**140**	***322.32***	***24.94***
Anhe_1_6_4	207	5.51	0.181	18.484	7.39%	0.127	10.24%	**1920**	**190**	***309.06***	***23.26***
Anhe_1_6_5	234	7.94	0.126	20.833	7.29%	0.074	5.11%	**1038**	**100**	***294.11***	***21.19***
Anhe_1_6_6	284	7.12	0.140	20.000	6.20%	0.073	4.27%	**1008**	**88**	***306.87***	***18.79***
Anhe_1_6_7	153	10.57	0.095	19.724	6.51%	0.084	4.05%	**1297**	**74**	***306.67***	***19.73***
Anhe_1_6_8	105	0.81	1.230	12.821	6.54%	0.130	5.38%	**2076**	**95**	***484.00***	***30.00***
Anhe_1_6_9	53	0.72	1.383	13.333	5.73%	0.096	5.29%	**1535**	**100**	***469.00***	***26.00***
Anhe_1_6_10	74	0.84	1.198	14.620	5.56%	0.058	4.34%	**519**	**100**	***426.70***	***23.00***
Anhe_1_6_11	2,180	3.39	0.295	17.391	5.91%	0.087	5.38%	**1361**	**100**	***345.65***	***20.23***
Anhe_1_6_12	3,690	2.97	0.337	18.083	6.87%	0.078	5.81%	**1116**	**120**	***336.79***	***22.86***
Anhe_1_6_13	26	1.12	0.897	5.992	5.57%	0.076	4.10%	**1083**	**82**	***994.00***	***50.00***
Anhe_1_6_14	37	1.08	0.926	5.889	5.71%	0.073	4.10%	**1020**	**80**	***1010.00***	***53.00***
Anhe_1_6_15	53	1.16	0.864	5.875	5.58%	0.075	3.75%	**1058**	**77**	***1013.00***	***53.00***

Appendix II. (continued) LA-SF-ICP-MS analyses of zircons

Euhedral Zircons				Radiogenic Ratios				Ages (Ma)			
					2 σ		2 σ		2 σ		2 σ
Sample (n=18)	U (ppm)	Th (ppm)	$^{232}Th/^{238}U$	$^{238}U/^{206}Pb$	(%) err	$^{207}Pb/^{206}Pb$	(%) err	$^{207}Pb/^{206}Pb$	abs err	$^{206}Pb/^{238}U$	abs err
Euhe_1_to_7_1	322	10.80	0.09	20.5339	6.78%	0.084	5.47%	**1266**	**110**	***294.71***	***19.8***
Euhe_1_to_7_2	251	13.53	0.07	20.5761	6.58%	0.081	4.71%	**1216**	**94**	***295.42***	***19.2***
Euhe_1_to_7_3	336	12.17	0.08	21.6920	7.38%	0.098	7.22%	**1560**	**130**	***274.15***	***20.1***
Euhe_1_to_7_4	746	10.76	0.09	22.1729	6.65%	0.065	4.33%	**752**	**89**	***279.95***	***18.4***
Euhe_1_to_7_5	662	9.48	0.11	22.2222	7.11%	0.077	4.97%	**1108**	**110**	***275.25***	***19.4***
Euhe_1_to_7_6	816	9.97	0.10	21.9780	6.81%	0.072	3.88%	**985**	**80**	***279.77***	***18.8***
Euhe_1_to_7_7	293	13.75	0.07	20.7039	7.04%	0.083	4.82%	**1279**	**92**	***292.73***	***20.4***
Euhe_1_to_7_8	111	13.31	0.08	16.0514	7.70%	0.259	4.64%	**3240**	**78**	***292.25***	***24.1***
Euhe_1_to_7_9	240	13.57	0.07	22.3714	8.05%	0.086	4.64%	**1341**	**94**	***270.10***	***21.5***
Euhe_1_to_7_10	153	15.58	0.06	19.8413	7.54%	0.084	5.22%	**1276**	**98**	***304.76***	***22.7***
Euhe_1_to_7_11	162	18.69	0.05	19.9203	7.37%	0.096	6.91%	**1520**	**120**	***299.25***	***21.9***
Euhe_1_to_7_12	367	0.15	6.67	10.4058	7.60%	0.517	5.61%	**4289**	**81**	***591.00***	***43.0***
Euhe_1_to_7_13	90	5.70	0.18	18.0180	6.67%	0.199	5.04%	**2800**	**90**	***286.46***	***19.9***
Euhe_1_to_7_14	152	6.38	0.16	18.7970	6.02%	0.159	8.18%	**2420**	**130**	***290.92***	***18.3***
Euhe_1_to_7_15	298	8.40	0.12	19.7628	6.13%	0.101	5.27%	**1612**	**97**	***299.62***	***18.3***
Euhe_1_to_7_16	351	10.07	0.10	20.8768	6.05%	0.077	4.17%	**1113**	**85**	***292.62***	***17.5***
Euhe_1_to_7_17	344	4.84	0.21	15.8228	7.91%	0.286	14.69%	**3100**	**280**	***283.10***	***31.2***
Euhe_1_to_7_18	655	1.37	0.73	14.4300	5.63%	0.067	5.26%	**807**	**110**	***431.90***	***24.0***

Appendix II. (continued) LA-SF-ICP-MS analyses of zircons

Standards				Radiogenic Ratios				Ages (Ma)			
					2 σ		2 σ		2 σ		2 σ
Sample (n=19)	U (ppm)	Th (ppm)	$^{232}Th/^{238}U$	$^{238}U/^{206}Pb$	(%) err	$^{207}Pb/^{206}Pb$	(%) err	$^{207}Pb/^{206}Pb$	abs err	$^{206}Pb/^{238}U$	abs err
Ou49127_1	436	0.69	1.45	46.4900	6.04%	0.0501	4.59%	**188**	**97**	***136.97***	***8.23***
Ou49127_2	435	0.77	1.31	46.6418	6.53%	0.0482	4.98%	**131**	**100**	***136.85***	***8.88***
Ou49127_3	420	0.67	1.49	45.9982	5.52%	0.0555	4.68%	**416**	**100**	***137.51***	***7.55***
Ou49127_4	272	1.08	0.93	45.5789	6.84%	0.0668	9.58%	**770**	**190**	***136.83***	***9.36***
Ou49127_5	351	0.93	1.08	44.9438	6.29%	0.0571	5.25%	**480**	**110**	***140.43***	***8.79***
Ou49127_6	288	1.01	0.99	44.6628	6.25%	0.0627	5.10%	**706**	**100**	***140.33***	***8.73***
Z_Plesovice_1	10,150	1.23	0.81	16.9492	8.14%	0.0559	6.26%	**410**	**130**	***368.67***	***29.51***
Z_Plesovice_2	20,900	1.75	0.57	18.4843	9.80%	0.0541	6.10%	**360**	**130**	***339.29***	***32.72***
Z_Plesovice_3	15,140	0.83	1.20	17.6678	6.54%	0.0549	4.74%	**400**	**110**	***354.36***	***22.80***
Z_Plesovice_4	12,100	2.39	0.42	20.6186	8.25%	0.0535	5.61%	**360**	**130**	***304.92***	***24.80***
Z_Plesovice_5	5,650	2.97	0.34	18.6220	6.33%	0.0556	4.50%	**445**	**99**	***336.21***	***20.97***
Z_91500_1	79	2.63	0.38	5.7471	6.32%	0.0752	5.59%	**1072**	**100**	***1032.00***	***59.00***
Z_91500_2	76	2.63	0.38	5.5127	7.17%	0.0753	5.44%	**1050**	**110**	***1073.00***	***68.00***
Z_91500_3	87	2.81	0.36	5.5525	6.66%	0.0747	5.62%	**1059**	**110**	***1066.00***	***64.00***
Z_91500_4	77	2.61	0.38	5.5371	4.98%	0.0750	4.00%	**1067**	**80**	***1074.00***	***49.00***
Z_91500_5	80	2.47	0.40	5.4259	4.77%	0.0740	4.05%	**1041**	**79**	***1090.00***	***48.00***
Z_91500_6	84	3.12	0.32	5.8445	7.01%	0.0740	4.19%	**1043**	**78**	***1018.00***	***68.00***
Z_91500_7	78	2.60	0.38	5.5991	7.28%	0.0765	3.79%	**1110**	**80**	***1059.00***	***71.00***
Z_91500_8	79	2.65	0.38	5.5310	5.53%	0.0740	3.78%	**1050**	**82**	***1071.00***	***55.00***

	Mass	SiO_2	Al_2O_3	Fe_2O_3	MnO	MgO	CaO	Na_2O	K_2O	TiO_2	P_2O_5	LOI	Total	Ag	Al	As	Au	Ba	Be	Bi
	g	*%*	*%*	*%*	*%*	*%*	*%*	*%*	*%*	*%*	*%*	*%*	*%*	*ppm*	*%*	*ppm*	*ppb*	*ppm*	*ppm*	*ppm*
RRE-15	31.5	75.19	12.51	1.87	0.052	0.2	0.79	3.03	5.05	0.186	0.05	0.74	99.67	< 0.05	6.46	2.6	6	384	3.2	8
RRE-31	31.3	76.92	12.24	1.66	0.052	0.19	0.53	3.19	4.94	0.145	0.05	0.42	100.3	0.08	6.6	< 0.5	< 2	197	4.8	0.9
RRE-32B	31.3	77.15	12.41	1.78	0.044	0.14	0.46	2.92	4.93	0.166	0.02	0.59	100.6	< 0.05	6.62	< 0.5	< 2	233	5	0.2
RRE-110	30.4	77.51	11.74	1.38	0.05	0.05	0.28	3.35	4.51	0.068	< 0.01	0.45	99.39	0.58	6.45	1.4	< 2	27	6.8	0.2
RRE-149	30.2	76.69	12.27	1.72	0.043	0.19	0.52	2.79	4.82	0.177	0.03	0.82	100	0.48	6.86	< 0.5	< 2	156	5.6	0.2
FRE-18	32.6	76.56	12.57	1.52	0.047	0.16	0.49	3.04	5.03	0.167	0.07	0.59	100.2	< 0.05	6.46	0.8	< 2	119	4.9	< 0.1

	Mass	Br	Ca	Cd	Ce	Co	Cr	Cs	Cu	Dy	Er	Eu	Fe	Ga	Gd	Ge	Hf	Hg	Ho	In
	g	*ppm*	*%*	*ppm*	*ppm*	*ppm*	*ppm*	*ppm*	*ppm*	*ppm*	*ppm*	*ppm*	*%*	*ppm*	*ppm*	*ppm*	*ppm*	*ppb*	*ppm*	*ppm*
RRE-15	31.5	< 0.5	0.61	< 0.1	117	1.4	26	2.39	26.4	6.9	3.9	0.8	1.23	15.8	7.6	< 0.1	3	< 10	1.4	0.1
RRE-31	31.3	< 0.5	0.4	< 0.1	106	1.2	23	2.2	7.2	32	15.5	2.4	1.04	18.8	36.7	< 0.1	1.9	< 10	5.8	< 0.1
RRE-32B	31.3	< 0.5	0.35	< 0.1	130	1.2	32	2.7	3.6	37.3	18.4	3.3	1.37	18.1	40.4	< 0.1	1.5	< 10	6.8	< 0.1
RRE-110	30.4	< 0.5	0.22	< 0.1	67.5	0.5	31	2.84	4.6	18.6	10.2	0.2	0.94	22	16.8	< 0.1	4.4	< 10	3.6	0.1
RRE-149	30.2	< 0.5	0.43	< 0.1	60	1.3	19	6.48	2.5	9.7	6	0.5	1.11	19.3	7.3	0.2	3.6	< 10	2	< 0.1
FRE-18	32.6	< 0.5	0.38	< 0.1	101	1.5	22	4.38	6.6	6.4	4.9	0.2	1.02	19.1	4.4	0.3	3.2	< 10	1.5	< 0.1

Appendix III. (continued) Geochemical analyses of the Alabama LICG

	Mass	Ir	K	La	Li	Lu	Mg	Mn	Mo	Na	Nb	Nd	Ni	P	Pb	Pr	Rb	Re	S	Sb
	g	*ppb*	*%*	*ppm*	*ppm*	*ppm*	*%*	*ppm*	*ppm*	*%*	*ppm*	*ppm*	*ppm*	*%*	*ppm*	*ppm*	*ppm*	*ppm*	*%*	*ppm*
RRE-15	31.5	< 5	3.9	59.2	22.3	0.24	0.12	371	2	2.16	1.9	52.4	0.9	0.012	27.7	14.5	157	< 0.001	0.03	0.5
RRE-31	31.3	< 5	4.27	273	32	0.86	0.1	379	1	2.25	5.9	245	3.1	0.007	33.8	68.5	206	< 0.001	< 0.01	< 0.1
RRE-32B	31.3	< 5	4.69	322	37.9	1.03	0.08	371	< 1	2.01	7.1	317	0.7	0.009	34.7	90.2	210	< 0.001	< 0.01	< 0.1
RRE-110	30.4	< 5	4.02	64	33.6	0.67	0.03	428	1	2.34	56	73.4	< 0.5	0.002	39.5	19.7	306	< 0.001	< 0.01	< 0.1
RRE-149	30.2	< 5	4.37	47.8	50.8	0.43	0.12	369	< 1	2	42.2	52.9	1.5	0.01	23.1	16.8	259	< 0.001	< 0.01	< 0.1
FRE-18	32.6	< 5	4.37	25.9	35.7	0.41	0.09	337	5	2.19	5.6	22.9	0.9	0.01	26.5	7.1	265	< 0.001	< 0.01	0.2

	Mass	Sc	Se	Sm	Sn	Sr	Ta	Tb	Te	Th	Ti	Tm	U	V	W	Y	Yb	Zn	Zr
	g	*ppm*	*ppm*	*ppm*	*ppm*	*ppm*	*ppm*	*ppm*	*ppm*	*ppm*	*%*	*ppm*	*ppm*	*ppm*	*ppm*	*ppm*	*ppm*	*ppm*	*ppm*
RRE-15	31.5	4.1	< 0.1	8.8	5	47.7	< 0.1	1.1	0.1	18.4	0.09	0.6	3.8	6	< 1	38.3	4.4	38	77
RRE-31	31.3	5.5	< 0.1	48.5	6	27.2	< 0.1	5.5	< 0.1	29.9	0.09	2.3	9	5	< 1	148	16.9	54	43
RRE-32B	31.3	4.6	< 0.1	64.9	5	28.2	< 0.1	6.3	< 0.1	21.5	0.1	2.8	8.8	7	< 1	166	21.7	50.4	43
RRE-110	30.4	7.1	< 0.1	17.5	12	6.8	2.2	2.9	< 0.1	36.7	0.05	1.6	10	2	< 1	96.8	12	45.8	79
RRE-149	30.2	4.7	< 0.1	11.1	6	39.5	1	1.4	0.7	39.2	0.12	1	10.1	9	< 1	50.2	7.9	15.9	88
FRE-18	32.6	4.8	< 0.1	4.6	6	28	< 0.1	0.9	0.2	38.4	0.08	0.8	12.5	6	< 1	38.9	6.7	20.5	77

Appendix IV. Geochemical analyses of the Georgia LICG

	SiO_2	Al_2O_3	Fe_2O_3	MnO	MgO	CaO	Na_2O	K_2O	TiO_2	P_2O_5	Total
	%	%	%	%	%	%	%	%	%	%	%
1A	67.086	15.085	4.7039	0.0591	1.6427	3.08	4.389	1.89	0.5572	0.1338	98.628
1B	68.369	16.801	4.2606	0.0739	1.7392	3.61	4.7934	2.1546	0.5773	0.1224	102.5
2A	75.172	15.448	2.5172	0.0609	0.5741	1.78	4.5993	3.5319	0.2671	0.0738	104.03
2B	75.942	13.275	2.2092	0.0682	0.5512	1.45	3.8228	3.4066	0.2313	0.0046	100.96
3	67.856	15.618	4.6524	0.0656	1.5505	3.34	4.4618	1.9529	0.5101	0.093	100.1
4A	70.209	16.401	2.9138	0.0522	1.5432	3.53	4.7637	1.8161	0.4773	0.1242	101.83
4B	70.166	15.875	3.9146	0.0602	1.5313	3.46	4.3863	2.2675	0.4837	0.0843	102.23
5	77.653	14.832	1.8264	0.0292	0.6126	2.33	4.5858	1.9669	0.2126	0.0284	104.08
6	70.551	15.38	4.6524	0.0648	1.5339	3.22	4.2461	1.9789	0.5732	0.1389	102.34

Appendix V. Discriminatory analysis of the LICG after Shaw (1972)

Sample	SiO_2	FeO	MgO	CaO	Na_2O	K_2O	0.21 SiO_2	0.32 FeO	0.98 MgO	0.55 CaO	1.46 Na_2O	0.54 K_2O	DF*	Sed. vs. Ig. Protolith
RRE-15	75.19	1.87	0.2	0.79	3.03	5.05	15.79	0.60	0.20	0.43	4.42	2.73	1.44	Igneous
RRE-31	76.92	1.66	0.19	0.53	3.19	4.94	16.15	0.53	0.19	0.29	4.66	2.67	1.19	Igneous
RRE-32B	77.15	1.78	0.14	0.46	2.92	4.93	16.20	0.57	0.14	0.25	4.26	2.66	0.71	Igneous
RRE-110	77.51	1.38	0.05	0.28	3.35	4.51	16.28	0.44	0.05	0.15	4.89	2.44	1.15	Igneous
RRE-149	76.69	1.72	0.19	0.52	2.79	4.82	16.10	0.55	0.19	0.29	4.07	2.60	0.56	Igneous
FRE-18	76.56	1.52	0.16	0.49	3.04	5.03	16.08	0.49	0.16	0.27	4.44	2.72	1.14	Igneous
1A	67.09	4.70	1.64	3.08	4.39	1.89	14.09	1.51	1.61	1.69	6.41	1.02	2.36	Igneous
1B	68.37	4.26	1.74	3.61	4.79	2.15	14.36	1.36	1.70	1.99	7.00	1.16	3.16	Igneous
2A	75.17	2.52	0.57	1.78	4.60	3.53	15.79	0.81	0.56	0.98	6.71	1.91	2.89	Igneous
2B	75.94	2.21	0.55	1.45	3.82	3.41	15.95	0.71	0.54	0.80	5.58	1.84	1.46	Igneous
3	67.86	4.65	1.55	3.34	4.46	1.95	14.25	1.49	1.52	1.84	6.51	1.05	2.59	Igneous
4A	70.21	2.91	1.54	3.53	4.76	1.82	14.74	0.93	1.51	1.94	6.96	0.98	3.13	Igneous
4B	70.17	3.91	1.53	3.46	4.39	2.27	14.73	1.25	1.50	1.91	6.40	1.22	2.49	Igneous
5	77.65	1.83	0.61	2.33	4.59	1.97	16.31	0.58	0.60	1.28	6.70	1.06	1.99	Igneous
6	70.55	4.65	1.53	3.22	4.25	1.98	14.82	1.49	1.50	1.77	6.20	1.07	1.67	Igneous

* Discriminant function calculated by DF = 10.44 - (0.21*SiO_2) - (0.32*FeO) - (0.98*MgO) + (0.55*CaO) + (1.45*Na_2O) + (0.54*K_2O). See Shaw (1972) for more details.

Geologic Map of the 1:24,000 Roanoke East, Alabama, Quadrangle

By: Rylleigh P. Harstad and Mark G. Steltenpohl
Department of Geosciences, Auburn University, Auburn, AL 36849

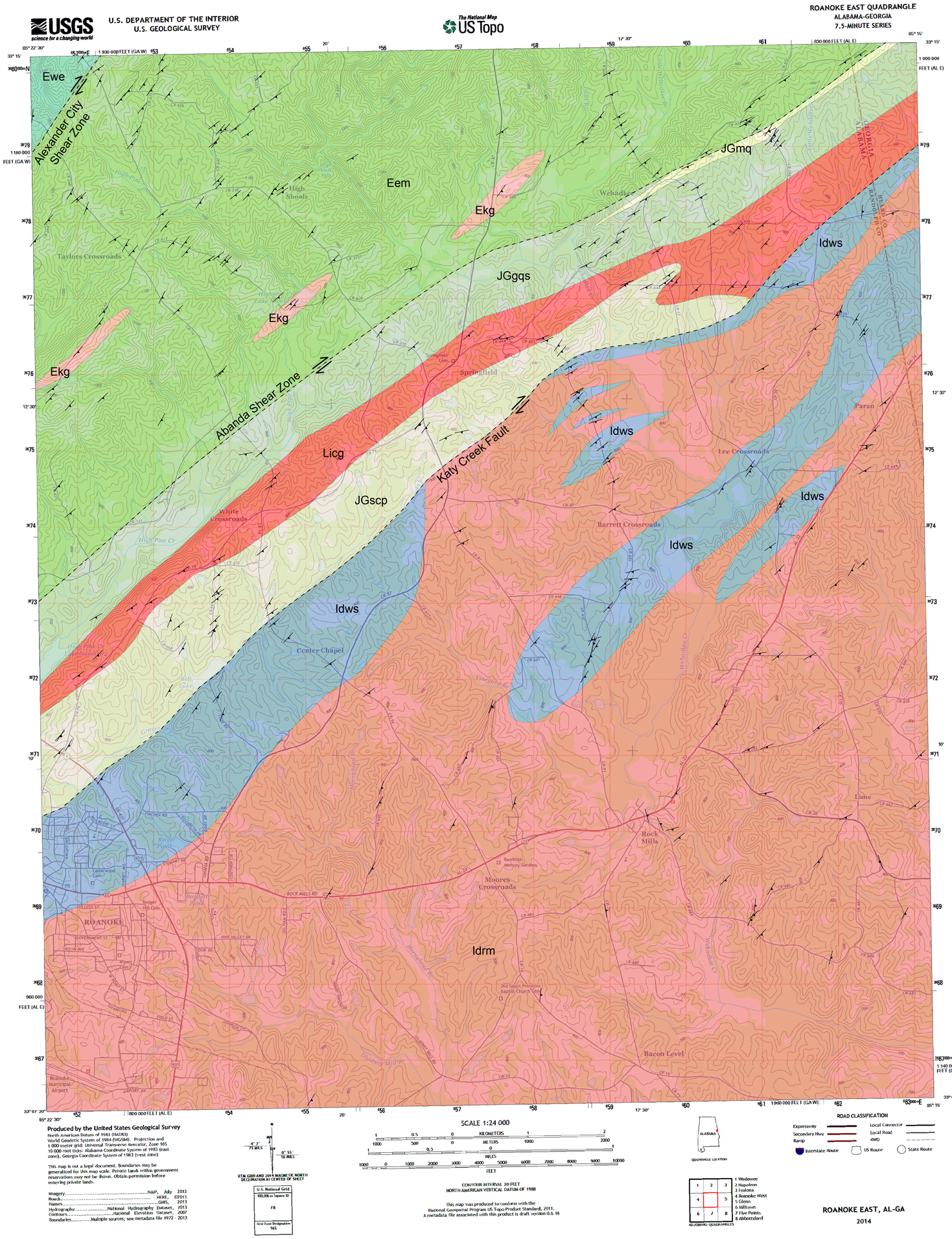

Basemap is a GeoTiff obtained from the
USGS TopoView (2015) website: http://ngmdb.usgs.gov/maps/TopoView/
Map produced using ESRI ArcGIS 10.2
31 August 2016

Funding provided by the National Cooperative Geologic Mapping Program (NCGMP) and the United States Geologic Survey (USGS) through an EDMAP Grant (USGS-G15A500005)

LEGEND

Lithologic Units

Inner Piedmont

Dadeville Complex

Idrm Rock Mills Granite Gneiss — Well-foliated, medium- to coarse-grained granitic gneiss containing biotite, muscovite, quartz, potassium feldspar, and varying minor amounts of epidote and garnet.

Idws Waresville Schist — Interlayered felsic and mafic schists. Felsic schists are fine- to medium-grained and contain varying amounts of quartz, plagioclase, potassium feldspar, sericite, and minor pyrite. Mafic layers comprise amphibole-bearing schist and thinly banded to massive amphibolite. Locally, muscovite schists with opaques are interlayered with the felsic and mafic schists.

Katy Creek Fault

Brevard Shear Zone

Jacksons Gap Group

Licg Long Island Creek Gneiss — Medium- to coarse-grained, moderately- to well-foliated epidote-muscovite-biotite-quartz-feldspar-gneissic granite. Intrudes the units of the Jacksons Gap Group. Tectonostratigraphic position not understood.

JGscp Sericite-Chlorite Phyllite — Fine- to medium-grained, well-foliated, locally graphitic phyllites that contain varying amounts of muscovite, sericite, chlorite, quartz, and garnet. Locally interlayered with garnetiferous schists similar to those within JGgqs.

JGgqs Garnetiferous Quartz Schist — Locally graphitic, fine- to medium-grained garnet-quartz-biotite-sericite schist.

JGmq Micaceous Quartzite — Fine- to medium-grained, well-foliated, micaceous quartzite containing varying amounts of muscovite, biotite, sericite, quartz, and feldspar.

Abanda Shear Zone

Eastern Blue Ridge

Emuckfaw Group

Ekg Kowaliga Gneiss — Medium- to coarse-grained augen gneiss containing quartz, potassium feldspar, plagioclase, biotite, and muscovite.

Eem Emuckfaw Group — Undifferentiated package of locally graphitic and garnetiferous muscovite-biotite-quartz-feldspar schist, fine-grained muscovite-biotite-quartz-feldspar metawacke, and thin (<0.5 m), rare fine-grained banded amphibolite.

Alexander City Shear Zone

Wedowee Group

Ewe Wedowee Group — Graphitic garnetiferous muscovite-biotite-quartz-feldspar schist interlayered with banded to massive amphibolite.

Structural Symbols

- Contact
- Fault/Shear Zone
- Dextral Strike-Slip Movement
- S_0/S_1 Metamorphic Foliation